Patterns and drivers of development in a west Amazonian peatland during the late Holocene

Thomas J. Kelly[a], Ian T. Lawson[b, *], Katherine H. Roucoux[b], Timothy R. Baker[c], and Euridice N. Honorio Coronado[d].

[a] Department of Civil and Environmental Engineering, Imperial College London, South Kensington Campus, London SW7 2AZ

[b]School of Geography and Sustainable Development, University of St Andrews, Irvine Building, North Street, St Andrews, KY16 9AJ, UK

[c]School of Geography, University of Leeds, Leeds, LS2 9JT, UK

[d]Instituto de Investigaciones de la Amazonía Peruana, Iquitos, Av. José A. Quiñones km. 2.5 - Apartado Postal 784, Loreto, Peru

* Corresponding author. E-mail address: itl2@st-andrews.ac.uk (Dr Ian Lawson).

Abstract

Amazonian peatlands sequester and store large amounts of carbon below ground and contribute to regional biodiversity. They also present an outstanding opportunity for palaeoecological research. This study uses multiple peat cores to improve our understanding of the long-term development of a peatland (Quistococha) in Peruvian Amazonia, by providing a reconstruction of the spatial patterns of vegetation change and peat accumulation over time across the site. Peat cores taken along transects totalling c. 5 km were used to establish the peat thickness and visible stratigraphy. Of 29 new peat cores, four were selected for pollen analysis, supported by 15 radiocarbon dates. These complement two existing published pollen records from the site, from a peat core and a lake sediment core. Our study shows that peat initiation occurred across the site in the form of primary mire formation between 2,400 and 1,900 cal yr BP. Following peat initiation, five broadly similar phases of vegetation development are recorded in all the pollen sequences: Amazon floodplain, herbaceous sedge fen, mixed angiosperm flooded forest, mixed palm swamp, *Mauritia*-dominated palm swamp. In detail, there are differences in the pattern and timing of vegetation change between the sequences. Much of this spatial variation is likely to be the result of the underlying substrate topography. In addition, we find that the difference in vegetation composition between core sites was greater during the early stages of peat accumulation at Quistococha than it is today. Such spatial and temporal variability has

significant implications for computer modelling of carbon accumulation in tropical peatlands and, consequently, our understanding of their role in the global carbon cycle. Our findings highlight key challenges for numerical modelling on Holocene timescales, namely the difficulty in quantifying long-term variations in primary productivity, the variable influence of sediment input on carbon accumulation during the early stages of peatland formation, and the difficulty of modelling water tables in sites with variable underlying topography.

Key words: palaeoecology, mire formation, Peru, palynology, vegetation succession.

1. Introduction

Peatlands within the tropical latitudes are estimated to cover 441,000 km^2 and store about 120 Pg of carbon (Page et al., 2011; Dargie et al. 2017), which makes them one of the largest stores of terrestrial carbon in the tropics, about half as large as the carbon storage of biomass in *terra firme* forests (c. 247 Pg C; Saatchi et al., 2011). The largest and deepest peatlands occurring at tropical latitudes are in Southeast Asia (Page et al., 2011), but recent research has shown that there are substantial peat accumulations throughout the tropics. In Amazonia, the largest area of peatlands yet identified is the Pastaza-Marañón Foreland Basin (PMFB), northeast Peru (Lähteenoja et al., 2009, 2011, 2012; Draper et al., 2014). The PMFB peatlands are estimated to cover an area of c. 35,600 km^2, and store c. 3.14 Pg of carbon (Draper et al., 2014), which is equivalent to about half of the total carbon stored above ground in forests throughout the whole of Peru. Although they are often regionally important emitters of methane, and peatlands in the Amazon are no exception, under natural conditions undisturbed peatlands are net carbon sinks (Teh et al., 2017). For this reason, Amazonian peatlands are becoming a focus for carbon conservation, although there is also a strong case to be made for protecting them for their socio-cultural and biodiversity values (Roucoux et al., 2017). Palaeoecology has an important role to play in the PMFB and in intact tropical peatlands more generally, in helping to build the science base needed to understand (i) how and why peat carbon is distributed (unevenly) across the landscape, (ii) the robustness of different types of peatlands as carbon stores and sinks, and (iii) how plant and animal species of conservation or socio-cultural value come to have their present-day distribution. Understanding successional change is of primary importance in modelling future peatland carbon dynamics; due to the connection with net primary production, succession is a key element to include in peatland models (e.g. Baird et al., 2012). Where models fail to simulate observed changes in peatland carbon accumulation during the Holocene in Amazonia, the long-term view of ecohydrological dynamics given by palaeoecology has the potential to provide explanations (Wang et al., 2018).

With these wider aims in mind we have undertaken a series of studies of PMFB peatlands. This paper reports a multiple-core study from a palm swamp, Quistococha. This 490 ha forested peatland, which contains peat up to 4.1 m thick (Lähteenoja et al., 2009a), is thought to occupy an abandoned arm of the Amazon river (Räsänen et al. 1991), the main stem of which has since migrated 12 km to the east across its floodplain. Quistococha has increasingly become a focus for research, with more published papers on its present and past environment than any other peatland site in the region. Recent studies have measured greenhouse gas emissions (Teh et al. 2017), examined the testate amoebae found in the present-day lake (Patterson et al., 2015), and assessed the impact of *Mauritia flexuosa* harvesting on aboveground carbon stocks (Bhomia et al., 2018). The first numerical models for Amazonian peatlands have also been validated using data from Quistococha (Wang et al., 2018). An initial appraisal of peat carbon storage and chemistry at Quistococha was made by Lähteenoja et al. (2009a,b), followed by more detailed multiple-proxy analyses of a single peat core by Roucoux et al. (2013) and Lawson et al. (2014). Previous work has also been undertaken on sediment sequences from the lake at the centre of the site by Räsänen et al. (1991) and Aniceto et al. (2014a,b), providing estimates of when the site was abandoned by the Amazon river channel, and of carbon accumulation rates in the lake sediments. A palaeoecological study of a lake sequence by Kelly et al. (2018) has also provided a pollen record covering the last c. 4500 years of the site's history, and refined earlier radiocarbon chronologies. However, while our understanding of this peatland (and other peatlands like it) has improved considerably in the last ten years, much remains unknown. An important gap in our knowledge is the spatial pattern of peatland development and vegetation change since this is essential if we are to understand the mechanisms and drivers of peatland development and associated carbon accumulation. The classical model of peat bog formation in a shallow aquatic basin is characterised in outline by strong directionality from open water, through minerotrophic fen, and potentially to ombrotrophic bog communities, as the accumulation of sediment and peat raises the surface above the local groundwater table (e.g. Walker 1970). This pattern and its drivers, autogenic and allogenic, have been widely studied in temperate and boreal peatlands (e.g. Klinger, 1996; Bunting and Warner, 1998; Bauer et al., 2003; Ireland et al., 2012). However, the extent to which the classical model (and variations on it) apply in Amazonian peatlands is not yet known as spatial patterns in vegetation change, their relationship to basin mire development, and the role of autogenic and allogenic factors, remain to be examined in detail in these systems.

Here we integrate the existing data from Quistococha with new datasets, including four new pollen records from cores taken across the peatland and a substantial set of new down-core and basal dates, to improve our understanding of peatland development, specifically: (1) How did the mire form, and (2) how did the mire and its vegetation then develop over time and space? Our analysis adds to the existing reconstruction of vegetation development at this site because it includes patterns of spatial heterogeneity that are not registered in the pollen signal from the existing single cores; one from the lake and one from the peatland. Typically low wind speeds within the forest mean that each peatland core has a small effective pollen source area and a highly local vegetation signal. Thus, the analysis of several cores taken across the forested site enables patterns of spatial heterogeneity in the vegetation to be registered. The pollen record from the lake (Kelly et al., 2018), with its much larger effective pollen source area, provides an integrated picture of the peatland and of the *terra firme* beyond, but of course does not provide spatial detail. In this paper, we use the pollen signal in four new peat core pollen sequences, in addition to the published records, to show how the peatland and its vegetation developed over time and space.

2. Site description

The peatland at Quistococha is situated on the floodplain of the River Amazon 8 km south of the city of Iquitos (Figure 1). The Landsat imagery indicates that there may be peatland areas to the northeast (red colour), but these are separated from the main Quistococha peatland by a levee. The site was chosen for detailed study both for its ease of access and because, on floristic grounds, it represents one of the most common types of peatland ecosystem in western Amazonia (Lähteenoja et al., 2009a; Roucoux et al., 2013; Honorio et al., 2015; Draper et al., 2017). The vegetation is closed canopy palm swamp, dominated by three tree species, *Mauritia flexuosa, Mauritiella armata* (both Arecaceae) and *Tabebuia insignis* (Bignoniaceae) (Roucoux et al., 2013). A (0.5 ha) plot-based census showed that the average height of all tree species was > 10 m, with *Mauritia flexuosa* the tallest species present (average 21 m). The three most common saplings (2.5–10 cm diameter) in the understorey were *Tabebuia insignis*, *Virola surinamensis* (Myristicaceae), and *Brosimum utile* (Moraceae) (Roucoux et al., 2013). While there is likely to be some variation in floristic composition across the site, remote sensing imagery shows that the prominent crowns of *Mauritia flexuosa* are present throughout the peatland. Aquatic plants on the lake today occupy small areas mostly within 10 m of the shoreline. There are small (c. 5 x 5 m) floating mats of Cyperaceae and Poaceae near the eastern

shoreline, and areas of floating Nympheaceae (aff. *Nymphaea amazonum*) around the lake margin.

The lake and peats lie on an impermeable substrate of clayey silt, thought to have been laid down by the Amazon (Räsänen et al. 1992; Lawson et al. 2014). The eastern margin of the peatland is bordered by a clay ridge which creates a low hydrological barrier between the peatland and the rest of the floodplain (Figure 2); to the west the peatland is bounded by a terrace of Miocene freshwater sands and silts. Artefacts found by archaeological excavations on the terrace northwest of the peatland suggest at least two periods of prehistoric occupation, between 1740-1880 and 2350-2690 cal yr BP (Rivas Panduro et al., 2006; Rivas Panduro, 2006). This is a site of regional archaeological importance and one of the few in Western Amazonia to have *terra preta* (anthropogenic dark earth) soils (Rivas Panduro et al., 2006)

Lähteenoja et al. (2009a) reported a basal radiocarbon age for the peat of 2320–2350 cal yr BP (1σ) (in core QT3 of that study at a depth of 3.90–4.00 m). Roucoux et al. (2013) obtained a statistically indistinguishable basal date of 2308-2056 cal yr BP (2σ) from 4.00 m depth in core QT-2010-1, taken at approximately the same location in the peatland. Lähteenoja et al. (2009b) and Lawson et al. (2014) showed that the inorganic chemistry of the upper peats (0–1.50 m) is consistent with a dominantly rain-fed system, with some groundwater input. We have observed two springs in the terrace that drain into the western edge of the peatland, and other groundwater flow may be occurring below the surface.

3. Material and Methods

3.1 Peat sampling

For this study, the peatland was sampled at 29 locations along c. 5 km of transect using a Russian-type corer (Jowsey, 1966), using parallel boreholes c. 2 m apart to collect a continuous sequence. The terrain on the southern part of the site was impassable due to c. 1 m deep standing water at the time of the survey, limiting the extent of the north-south transect. At each core site, coring continued downwards until the contact with the underlying clay was sampled. Cores were sub-sampled in the field at 16 cm intervals and stored in polythene bags; core sections containing the contact between the peat and the underlying clay were kept intact and wrapped in clingfilm and thick plastic sheeting. Core locations were recorded using a Garmin handheld GPS. Despite several attempts using various types of equipment, it was not possible to generate a precise estimate of elevation; SRTM and other remotely sensed data show no significant

variation in surface topography. All cores were stored under license at 4°C while awaiting analysis (Geography Department, University of Leeds; License held by T.R.

3.2 Sedimentological analysis

The peat and sediment composition was described in the field following Troels-Smith (1955), supported by additional laboratory checks for each of the 29 cores; those cores sampled for radiocarbon analysis were also examined using a low power stereo microscope.

Peat has varying definitions (Kelly et al., 2017a), but in this paper we discuss 'peat' as commonly operationally defined in the existing literature on tropical peatlands (i.e. >65% organic matter, thicker than 30cm; Dargie et al., 2017). However, as we will show, some of this 'peat' is in actual fact better described as gyttja (fine grained organic lake mud), deposited under fully aquatic conditions in open water.

For carbon and nitrogen analyses, samples of 1 cm^3 were dried at 105˚C, milled, then weighed into tin caps prior to analysis with a Eurovector Turboflash CNS combustion analyser. Vanadium pentoxide was used as a catalyst. The peat standard NJV942 was used with all sample batches. The experimental values for carbon and nitrogen were within 95% of the certified value for NJV942 for all sample runs. Loss-on-ignition was carried out to calculate the organic matter content; samples were dried overnight at 105˚C and dry weight calculated before combustion at 550 ˚C for two hours.

3.3 Pollen analysis

Fifteen pollen samples were analysed from core QT-2011-2, 24 from QT-2012-9, 12 from QT-2012-10 and 12 from QT-2012-18. Cores were selected to represent three different areas of the site, as well as to contrast cores with different peat thicknesses. Sampling resolution was typically 16 cm, with a finer resolution of 8 cm across the peat-clay contact, where variation in pollen assemblages between samples suggested that finer resolution was needed to register the pattern of vegetation change.

Sample preparation followed standard methods, including acetolysis and HF digestion where necessary (Faegri and Iversen, 1989). *Lycopodium* spore tablets were added as a "spike" to allow concentrations to be calculated (Stockmarr, 1971). Samples were mounted using silicone oil. Pollen, phytolith and charcoal analysis was undertaken using a Leica DMLS binocular microscope, routinely at 1000x under oil immersion. A minimum of 300 pollen sum grains were counted. The pollen sum excluded spores of the Pteridophyta and the pollen of the aquatic

plants such as *Pistia stratiotes* but included unknown pollen types (which make up only c. 5% of the total on average).

Identifications were based on modern reference material, the pollen atlases of Roubik and Moreno (1991) and Colinvaux et al. (1999), the Neotropical Pollen Database (Bush and Weng, 2006) and other literature (Absy, 1979; Nowicke and Takahashi, 2002; Van Geel, 2001; Burn and Mayle, 2008; Weber et al., 1999; Anderson, 1993; Walker and Walker, 1979; Dias Saba, 2007; Kelly et al, 2016). Optimal splitting by sum of squares was applied to produce independent pollen zonation schemes for each sequence in Psimpoll (Bennett, 2007) and the key taxa defining each zone were identified using indicator analysis (Dufrene and Legendre, 1997). Only pollen taxa that exceeded 5% in one or more samples were included in the analysis; all spores and aquatic taxa were excluded. The pollen data from all sequences were compiled and analysed using non-metric multidimensional scaling (NMDS: Minchin, 1987), to help identify common patterns among, and differences between, sequences. NMDS was performed on an abundance matrix of Bray-Curtis dissimilarities. NMDS and indicator analysis were undertaken in R 3.1.2 using the metaMDS function in vegan 2.3-2 and the indval function in labdsv 1.9-0 respectively (R Core Team, 2014; Oksanen et al., 2015; Roberts 2016).

3.4 Dating

For the new radiocarbon dates, bulk samples of 1–2 cm^3 in volume were prepared by sieving at 180 μm to ensure the removal of visible roots. The $\delta^{14}C$ and $\delta^{13}C$ content of the samples was determined by accelerator mass spectrometry (AMS) at the NERC Radiocarbon Facility in East Kilbride. Dates were calibrated using the INTCAL13 dataset (Reimer et al. 2013) in OxCal (Bronk Ramsey, 1995; Bronk Ramsey & Lee, 2013).

4. Results

4.1 Sedimentology and peat depth

The peat thicknesses along the four transects across the site are shown in Figure 2. The maximum peat thickness recorded anywhere on the site was 4.25 m, close to the location of QT-2010-1. Peat thickness varied considerably along, and between, the different transects. The present peat surface is gently undulating with occasional pools and, although we were not able to survey the elevation of the peat surface accurately, it seems likely that the basal topography undulates more than the peat surface because the differences in peat thickness are larger than the differences in surface height. Along transect A–A', peat thickness is consistently more than 1 m and the southernmost margin of the peatland was not reached. Along transect B–B' there

are two deeper parts to the basin separated by a buried ridge of clay. The minimum peat thickness sampled was 42 cm, close to the western margin of the peatland. Along transect C–C' peat thickness gradually decreases away from the lake (Figure 2) before meeting the levee which we inferred to represent the eastern boundary of the Quistococha peatland (Figure 1). However, a core beyond the levee confirms that this is not the limit of the peat accumulations in this area on the Amazon floodplain. Accumulations of peat consistently >3.0 m thick were found along Transect D–D' which runs approximately north-south along the eastern lake margin. Troels-Smith sediment logs for the four cores analysed in detail (QT-2011-2, QT-2012-9, QT-2012-10 and QT-2012) are presented in Figure 3. Five main types of material were observed:

- *Type 1:* Clayey silt with little organic content; underlies the peat at all locations sampled (Typically As3Ag1 or As4Ag+ using the Troels-Smith classification).
- *Type 2:* A mixture of clay, silt and organic matter ('muck' sensu Wüst et al. 2003); characterises the transition from clayey silt to peat (Typically As2Dg1Th1 or similar).
- *Type 3:* Organic material with few roots, typically slightly greenish in colour, and occasionally containing visible leaf fragments (typically Th1Sh1Ld2 or similar). This unit was similar to the material found accumulating in the lake close to its margin at the present day (Patterson et al., 2015).
- *Type 4:* Fibrous peat composed mainly of coarse palm and woody roots, with a well-humified matrix (typically Tl2 Sh2 Dh+).
- *Type 5:* Fibrous peat, as type 4 but markedly less humified material (typically Tl2 Dh1 Sh1); found in the upper part (< 1m depth) of all sequences.

Loss-on-ignition data, carbon and nitrogen concentrations are presented for four cores alongside the Troels-Smith logs in Figure 3. All four sequences exhibit a similar pattern of changing sediment type up-core. The transition from the underlying clayey silt to peat is gradual in three of the four cores (QT-2011-2, QT-2012-10, QT-2012-18), with organic content increasing over 20-30 cm. In core QT-2012-9 there is a relatively thick (91 cm) layer of mixed clay and organic matter (Type 2 above) with varying LOI values (50-90%). The upper part of the cores consisted of low-ash peat, typically >94% loss-on-ignition and >45wt% carbon; QT-2012-18 showed lower loss-on-ignition values (c. 85%). Nitrogen concentrations increase in the top 32 cm of all the cores; the increase in nitrogen concentration in the upper part of the sequences drives a reduction in C/N values.

4.2 Palynology

The pollen diagrams for selected taxa are presented in Figure 4, and are given in full in the supplementary information. Pollen preservation in the peat cores was good; the largest proportion of indeterminable pollen (13%) was found in the basal peat sample of QT-2011-2. There is an increase in damaged but identifiable grains towards the top of each sequence. Pollen concentrations (Figure 5) ranged from 17,700 to 1,376,000 grains cm^{-3}; the highest concentrations occur at 128 cm in QT-2012-10, attributable to an abundance of *Cecropia* pollen. Charcoal was largely absent from the peat sequences, and was present only as occasional fragments (see Supplementary Data). The pollen zones are described in Tables 4-7, and the main patterns are outlined here.

In QT-2011-2, zone Q2-A constitutes the sedimentological transition zone with increasing LOI, and the transition into the basal peats coincides with an abundance of *Symmeria paniculata* pollen (>40%) and moderately abundant Cyperaceae (11%). Zone Q2-B features peaks in Myrtaceae, Melastomataceae/Combretaceae, Rubiaceae, and Dalbergia. *Iriartea deltoideae* pollen is most abundant in this zone, although palms in general remain <10%. Cyperaceae also declines towards the top of zone Q2-B. Zones Q2-C and QC-D are marked by increased palm pollen abundance – mixed *Euterpe*-t. and *Mauritia*-t. in zone Q2-C and predominantly *Mauritia*-t in Q2-D.

In QT-2012-18, zone Q18-A is characterised as mixed clay and organics, and the transition to peat coincides with an interval of abundant *Symmeria paniculata* pollen (35% in the lower-most pollen sample), with Cyperaceae also persistently present (5-10%). Zone Q18-B includes peaks in Poaceae and Rubiaceae. In Q18-C, palms increase in abundance with a mixed *Euterpe*-t. and *Maurita*-t. assemblage, and in Q18-D *Euterpe*-t. declines, leaving *Mauritia*-t. as the dominant pollen taxon.

In QT-2012-10, the lowermost pollen zone Q10-A lies above the pure clay layer and includes the transition to peat (LOI >65%); it is characterised by persistent *Euterpe*-t. and *Mauritia*-t. palm pollen and a single peak in Myrtaceae. Zone Q10-B is defined by a single sample peak in *Cecropia* pollen (64%). Q10-C is characterised by an increase in palm pollen, with *Euterpe*-t. dominant in most samples in this zone (peak: 63%). In Q10-D, *Euterpe*-t. pollen declines to <5% and *Mauritia*-t. pollen dominates the assemblage, with *Alchornea* also consistently present.

In QT-2012-9, the basal sample in zone Q9-A lies just above the contact with the underlying clay in a part of the core characterised by low LOI (<25%). The pollen assemblage in this sample is comprised almost entirely of *Cecropia*, with some Cyperaceae and other taxa present in small quantities. The overlying pollen sample in Q9-A, taken from a section of the core where LOI >70%, is comprised predominantly of Cyperaceae pollen. In zone Q9-B, Cyperaceae is the dominant taxon in several samples (max.: 57%), with *Cecropia* remaining moderately abundant (>10% in most samples). Poaceae is also moderately abundant throughout this zone (>10%). In Q9-C, Cyperaceae initially declines in the basal zone and remains <10%, with the exception of a peak of 53% at 160 cm. This zone contains peaks in Myrtaceae, *Ilex* sp., Asteraceae, and *Psychotria*-t, and Poaceae is persistently present in low abundance (<10%). Zone Q9-D is defined by a single sample peak in *Ficus* pollen and is overlain by zone Q9-E where there is a small peak in *Euterpe*-t. pollen and *Mauritia*-t. gradually increases to become the dominant pollen taxon at the top of the core.

Some consistent patterns emerge among these cores. All four cores contain a high proportion of palm pollen in the top two zones, with *Mauritia*-t. typically increasing, then decreasing again as *Euterpe*-t. increases, before *Mauritia*-t. becomes increasingly abundant in the uppermost zone. Pollen grain size data suggest that the *Mauritia*-t. count includes an increasing proportion of *Mauritiella armata* pollen, which typically has smaller grains than the otherwise similar *Mauritia flexuosa* (Kelly et al., 2017b), in the upper 50 cm of cores QT-2011-2, QT-2012-9, and QT-2012-10. The persistent presence of *Tabebuia*-type pollen in these uppermost zones in most sequences probably reflects the taxon *T. insignis*, which is abundant at the site today (Roucoux et al., 2013).

The spinulose palm phytoliths counted down core can broadly be categorised as the 'globular echinate variant 1' type in the scheme developed for Andean phytoliths by Huisman et al. (2018). A representative SEM image is given in the Supplementary Information. Peaks in palm phytolith concentration (Figure 5) occur in all of the peat cores between 96 and 112 cm depth down core. This coincides with an increase in *Mauritia*-type pollen to >25 % of the pollen sum, and also with the main peak in *Mauritia*-t. pollen concentration in most of the cores. The highest concentration of palm phytoliths (1.86×10^6 phytoliths cm^{-3}) is in QT-2012-10.

There are, however, some notable differences between the four new pollen sequences, as also illustrated by their trajectories in the NMDS plots (Figure 7). *Symmeria paniculata* pollen is abundant in the basal zones of QT-2011-2 and QT-2012-18, and present but less abundant in

the other two cores. There are two distinct Myrtaceae peaks in core QT-2012-9, but only one in QT-2011-2 and QT-2012-10, and no peak in QT-2012-18 where Myrtaceae pollen was sparse throughout. A single-sample *Ficus* peak defines zone D of QT-2012-9, with no counterpart in any of the other cores. *Euterpe*-t. pollen is most abundant in QT-2012-10 and QT-2012-18, where it exceeds 50%; a clear *Euterpe*-t. peak is also visible in both QT-2012-9 and QT-2011-2 but at lower abundance (up to 13% in both cases). Poaceae sometimes exceeds 10% in the lower zones of QT-2012-9 and QT-2012-18 but is never abundant in the other two cores. In core QT-2012-10 there is a high single-sample peak in *Cecropia* just prior to the increase in palm pollen types.

4.3 Radiocarbon dates

The results of radiocarbon age determinations are presented in Table 2, and probability density functions for the calibrated peat basal dates are shown in Figure 8. The 15 new radiocarbon dates presented here include ten peat basal dates, and five further radiocarbon dates which were used to determine the peat accumulation rate and the timing of vegetation changes as recorded by the pollen. These add to the existing five dates from QT-3 (Lähteenoja et al., 2009), seven from QT-2010-1 (Roucoux et al. 2013) and 12 from QT-2010-3 (Kelly et al., 2018). The average maximum peat accumulation rate, as determined using peat basal dates, was 1.15 mm/yr, and the average minimum was 1.06 mm/yr (Table 3).

A basal sample from the shortest of the dated sequences (QT-2011-1) returned a date which, at 709-891 cal yr BP, is substantially younger than the ten other basal peat ages from the present study as well as the previously published dates (Lahteenoja et al., 2009; Roucoux et al., 2013). With this exception, the calibrated basal peat date ranges overlap substantially, with the overall 2σ range being 1897-2352 cal yr BP. The main expansion of *Mauritia*-t. is dated to 916-1174 cal yr BP in three sequences, and to 566-676 cal yr BP in QT-2012-9.

5. Discussion

5.1 Palaeoenvironmental reconstruction

Phase I: River channel to shallow water swamp

The history of the lake that remains today at the site has now been studied in detail in three separate palaeoenvironmental studies. The most recent work by Kelly et al. (2018), applied small-sample radiocarbon dating techniques using picked macrofossils and charcoal to overcome the reservoir effects that have affected bulk dates on minerogenic sediment in previous studies, producing older apparent ages for the abandonment of Quistococha (Räsänen

et al. 1992). The new dates suggested that the Quistococha basin was abandoned as an active meander of the Amazon sometime before 4500 cal yr BP, but that regular flooding by the Amazon continued to dominate deposition until c. 2400 cal yr BP (Kelly et al., 2018). These floodwater deposits, in the lake and under the peat across the site (QT1-A), consist of clayey silts, occasionally intercalated with more organic layers. In the lake core, pollen assemblages in the sediments deposited before c. 2,400 cal yr BP are overwhelmingly dominated by the pollen of *Cecropia* with Cyperaceae also an important component (Q3-A), and the clayey silts underlying the peatland have a similar pollen composition, but with less abundant Cyperaceae in the basal pollen zone (Roucoux et al., 2013). The two pollen records build a picture that resembles the shallow water swamps typical of recently abandoned meanders described by Kalliola et al. (1991b), with large areas of open water. *Cecropia* is abundant in disturbed riparian environments and its small, well-transported pollen grains are typically over-represented in lake contexts (Bush and Rivera, 1998, 2001; Gosling et al., 2009). Taken together, the evidence indicates that until c. 2400 cal yr BP the Quistococha basin was regularly flooded by the River Amazon. Aniceto et al. (2014) make the point that although carbon concentrations by weight in the clayey silts are low, the rapid sedimentation means that the clayey silts store a substantial amount of carbon. The available geochemical data (Aniceto et al., 2014; Lawson et al., 2014; Kelly et al., 2018) suggest that the organic matter preserved in the clayey silts largely came from fluvial sources, reworked from upland soils; *in situ* organic production seems to have been relatively unimportant during this period in terms of the overall carbon budget of the sediments.

Phase II: Herbaceous sedge fen and wooded swamp

The intercalated mineral and organic sediments at the base of several peat cores suggest a transitional period during which organic matter from overlying vegetation began to accumulate but with continued inputs of inorganic sediment from the Amazon. As the Amazon retreated and mineral inputs diminished, almost pure organic matter (>90% LOI) began to accumulate. This peat initiation began across the majority of the site between 2400-1900 yr BP, occurring slightly earlier in areas closer to the lake (2400-2100 yr BP) and later further from the lake (2100-1900) as indicated by the probability density functions generated for the radiocarbon dates (Figure 8). The relatively young date from the shallowest dated site (QT-2011-1) may also indicate that peat began to accumulate somewhat later on topographic highs in the substrate, e.g. on top of old meander ridges. Alternatively it is possible that this sample was contaminated by young carbon, despite efforts to remove roots by sieving.

The phase of abundant Cyperaceae recorded in QT-2012-9 and QT-2010-1 was interpreted as indicating either marginal fen or floating mat vegetation by Roucoux et al. (2013). Sedge communities are widespread in the PMFB and can occur on grounded peats as well as on floating mats (Draper et al., 2014; Draper, 2015); little is known of their ecology or precise palynological signature. This phase lasted for c. 100 years at QT-2010-1 (Roucoux et al., 2013). In the two shallowest peat cores studied here, the palynology of the basal peat layers suggests they were laid down under a less open, more wooded vegetation (e.g. Q2-A, Q18-A). In QT-2011-2, for example, entomophilous (Bawa et al., 1985) and therefore probably locally-derived Anacardiaceae pollen is very abundant in the basal sample (see Supplementary Data). Towards the base of QT-2012-10 (Q10-A) *Symmeria paniculata*, Myrtaceae, *Pouzolzia*, and Asteraceae pollen are all found at low percentages. *Symmeria* in particular is indicative of deep and persistent flooding with nutrient-poor water, while the low abundance of herbaceous taxa such as Cyperaceae, Poaceae and ferns, imply that this part of the site probably had a closed forest canopy at this time.

Patches of suitable habitat for *Mauritia* and/or *Mauritiella* were likely available near the lake from the onset of peat initiation. The transition from sporadic to continuous presence occurs c. 2000-2300 cal yr BP in the lake core which is approximately contemporaneous with peat initiation at ten of the eleven dated sites, but earlier than the local *Mauritia*-t. expansions recorded in the five peat pollen records. *Mauritia* and/or *Mauritiella* may not have been occupying areas of active peat accumulation, but other areas such as those around the western margin where *Mauritia* is still found at the present day growing on the slopes leading down to the lake, and in areas of clay substrate within 1 m elevation of the lake surface.

Phase III: Flooded forest

Both to the east and south of the lake, the pollen records indicate the expansion of forest at four of the core sites after the first c. 500 years of peat accumulation (the possible exception is QT-2012-18; see below). Most cores show an increase in the pollen of trees and shrubs typical of flooded forest such as *Alchornea*, Myrtaceae, and *Ilex* (Parodi and Freitas, 1990; Kalliola et al., 1991; Campbell et al., 1992; Wittman et al., 2006). In the longer cores (QT-2012-9 and QT-2010-1) there appear to be two Myrtaceae phases (e.g. Q9-C), separated by a phase with increased herbaceous vegetation such as Cyperaceae, Pteridophyte spores and, in QT-2012-9, an increase in *Mauritia*-t. The absence of a definite double peak in Myrtaceae and/or *Mauritia*-t. at some core sites is unlikely to be an artefact of the sampling resolution. This variation between sites may indicate that hydrological changes imposed on the site as a whole (e.g.

changes in flood amplitude) crossed ecologically-important thresholds at some locations but not others; for example, undulations in the peatland surface topography would create areas of varying flood depth. In support of this argument, for the earlier peak in *Mauritia*-t., where it occurs, grain size data suggest more variation in the ratios of *Mauritia* to *Mauritiella* in the different sequences for this earlier peak than for the later one. The differences in the ecology of these taxa are not well understood but our field observations suggest that they have subtly different edaphic and/or hydrological preferences. In particular, observations made by the authors in the field suggest that *Mauritiella armata* is more abundant in more deeply flooded environments than those in which *Mauritia flexuosa* is dominant; it has been suggested that *Mauritiella* occurs where flood amplitude is greater than 1–2 m (Junk et al., 2015).

At the southernmost site, QT-2012-18**,** which returned a relatively late date for peat initiation (1952–2111 cal yr BP), loss-on-ignition values remain below 90% in zone Q18-B indicating that there may also have been some continued sediment input, and perhaps deep/prolonged flooding. The vegetation during this phase remained more open than in the other records, with e.g. *Psychotria* (shrubs and small trees; Gentry, 1993) and Poaceae. In contrast to QT-2010-1, there is no strong evidence in this sequence for a separate seasonally flooded hard-wood forest phase; if one occurred, it must have been brief.

Phase IV: Mixed palm swamp

During this phase peat accumulation occurred under vegetation dominated by mixed palm trees or, at the location of QT-2010-1, mixed *Mauritia*-t. and *Ilex*. The occurrence of mixed *Mauritia flexuosa* and *Euterpe precatoria* forest is common today in permanently waterlogged areas flooded by black water (Parodi and Freitas, 1990; Kvist and Nebel, 2001). The expansion of *Mauritia*-t. appears more gradual in the lake core than in most of the peat cores but it shares a step-like expansion from c. 10% to 20%, dated to 541–707 cal yr BP, with an expansion dated to 566–676 cal yr BP recorded in QT-2012-9, the closest peat core to the present lake margin. This *Mauritia* expansion is later than that recorded in the other peat cores from the site (Figure 8), which centres around c. 1000 cal yr BP, and may mean that the increase in *Mauritia*-t. pollen in the lake record most closely reflects an expansion of *Mauritia* directly around the lake margins and resulting direct pollen deposition.

Elsewhere in Amazonia increased *Mauritia* abundance has been attributed to deliberate burning, such as in the Gran Sabana (Rull and Montoya, 2014). At Quistococha the very low concentrations of charcoal in the peat profiles suggest there was no *in situ* burning and that fire

did not play a role in the rise of *Mauritia* in this peatland (also see Roucoux et al., 2013), despite its potential resource value for those inhabiting the adjacent archaeological site (Hiraoka, 1999). However, to the east of the lake there is some evidence that the expansion of palms (e.g. Q10-D) may have followed a brief period of natural disturbance (e.g. Q10-C), as evidenced by the abundance of *Cecropia* and *Ficus*, both associated with early stages of riparian succession (Salo et al., 1986; Weng et al., 2004). In all of the peat cores, the increase in *Mauritia*-t. coincides with a peak in pollen and phytolith concentrations (Fig. 4), a feature also seen at another peatland in the region (at San Jorge, c. 30 km to the SSE of here) at about the same time (Kelly et al., 2017b). This may indicate a period of slow organic matter accumulation, as identified in the San Jorge sequence, but higher resolution dating will be required to test this proposal. Towards the latter part of this stage *Tabebuia* t. pollen becomes consistently present in several of the records probably representing *T. insignis* which today is very abundant at the site but which appears to be a poor pollen producer as it is under-represented in core-top and surface sample pollen assemblages (Kelly, 2015).

There is a difference in the forest composition between the shallow and deep peat areas, with *Mauritia*-t. being less abundant and *Euterpe*-t. more abundant on the areas of thinner peat (cf. Q9-E and Q10-C). There are two potential explanations. Firstly, the thin peat areas may have been more poorly drained; peat pools may have been more extensive in areas where the peat was thin and the surface was in closer proximity to the impermeable substrate (e.g. Comas et al., 2004). Secondly, the difference could be explained by greater nutrient availability in shallow peat (Frolking et al., 2010). For example, in QT-2012-10, a maximum of c. 70 cm of peat (not accounting for subsequent decay and compression) would have underlain the mixed palm swamp when it became established. The peat may have been shallow enough (<1 m) to allow nutrients transported in groundwater or leached from the mineral substrate to have reached the root-zone (Comas et al., 2004; Frolking et al., 2010).

Phase V: Mauritia flexuosa-dominated palm swamp (*Aguajal)*

In the final phase the pollen records all show a degree of consistency with *Mauritia*-t., likely representing mixed populations of *Mauritia* and *Mauritiella* in most cases, becoming increasingly dominant over other taxa such as *Euterpe* and *Ilex* (e.g. QT10-D, QT18-D). By this point (c. 400 cal yr BP onwards; Table 1), the accumulation of peat had progressed to the point where the topographic variation across most of the site had probably been subdued – as seen at the site today – and the vegetation was everywhere isolated from the mineral substrate. It is possible that this autogenic process has led to the convergence of vegetation composition

across the site which, at least along the transects we walked, is now dominated by *Mauritia flexuosa*, *Mauritiella armata*- and *Tabebuia insignis*.

In the lake sediment core there is an increase in *Cecropia* pollen from c. 20% to > 40% in the uppermost pollen zone which is not seen across the five records from the peatland itself. This feature likely reflects human impact and forest clearance on the terrace above the lake in recent decades (Kelly et al., 2018).

5.2 Implications for Amazonian peatland formation

The multi-core study of Quistococha provides important insights into the spatial development of the peatland and its vegetation; a feature of tropical peatlands that has only rarely been examined (e.g. Anderson, 1961; Phillips and Bustin, 1996). Following abandonment of the site by the Amazon, at least three scenarios for the infilling of the Quistococha basin with peat could be advanced: (i) Establishment of an oxbow lake and its gradual infilling by terrestrialization, from the edges towards the centre (as envisaged by Kalliola et al. 1991a on the basis of modern analogues); (ii) peat initiation at one site (perhaps the deepest), followed by slow lateral spread through paludification; (iii) primary mire formation across a waterlogged surface (see Sjörs, 1983). As discussed above, the basal peat dates indicate that at all but one of the locations we have sampled, peat began to accumulate within a window of c. 500 years. Unless peat could spread laterally over two kilometres within this interval, this would suggest that the third scenario is most likely. It seems that as soon as regular flooding from the Amazon ceased, organic material began to accumulate everywhere in the basin within 500 years, albeit with a slight lag towards the southern part of the site relative to areas closer to the lake. C/N ratios, lignin concentrations (Lawson et al., 2014; Kelly et al., 2018) and palynology all indicate that the organic material was dominantly terrestrial in origin from the outset, rather than organic-rich lake sediment (gyttja).

Many northern peatlands studies have shown continued, gradual (if episodic) expansion over the course of thousands of years (e.g. Bauer et al., 2003; Anderson et al., 2003; Ireland and Booth, 2011; Ireland et al., 2013). In some cases this expansion occurs across distances of 100–200 metres in around ten thousand years (e.g. Anderson et al., 2003). By contrast, the narrow window of peat initiation at Quistococha suggests that lateral expansion in the transects we studied was limited to the southern part of the site (across a distance of c. 500 m) and lasted no more than a few centuries. This suggests that primary mire formation is a more likely mechanism of peatland development in this case, with peat accumulation ‘switching on’ almost

simultaneously (within a 500 year window) in different areas. The persistence of the lake to the present day remains unexplained. It may occupy the deepest part of the basin, though this requires confirmation. Apart from a small area of sedge mat vegetation there is no evidence that it is undergoing terrestrialization; its shore consists in most places of a low cliff in the peat, bound by tree roots. It is possible that the lake has been kept open by a combination of a lack of macrophytic vegetation and by wave erosion (cf. Heinselman, 1963).

As a palm swamp peatland, Quistococha falls within the most abundant category (by area) of peatland in the PMFB recognised by Draper et al. (2014), but the extent to which the history of Quistococha is typical of other PMFB floodplain peatlands remains to be fully explored. Similar multiple-core palaeoenvironmental studies are also needed for raised mires, which are *a priori* likely to show different long-term spatial patterns. The pollen data from a single core from the domed site of San Jorge peatland, 30 km south of Quistococha, showed an unexpectedly complex pattern of change through time, including apparent 'reversals' in the succession (Kelly et al. 2017). Further work is needed to clarify the roles of fluvial action and regional climate change in the development of PMFB peatland ecosystems, particularly in terms of understanding the sensitivity of their carbon storage function. Reconstructions of water table changes based on testate amoebae transfer functions have suggested that at least one Peruvian peatland has responded substantially to recent climatically-driven hydrological changes (Swindles et al., 2018).

5.3 The influence of peatland substrate topography on vegetation

In regions where the ratio of precipitation to evaporation is not extremely high, peatlands are typically 'depressional' (Ireland et al., 2013), i.e. a waterlogged basin is required for peat to begin accumulating (Lähteenoja et al., 2009, 2012; Householder et al., 2012). To date, peat in lowland Amazonia has only been observed in depressional settings such as floodplains or forest hollows (Lähteenoja et al., 2009, 2013; Householder et al., 2012). In depressional peatlands elsewhere, basin shape has been shown to exert a strong influence on the development of the peatland and its associated vegetation (e.g. Walker, 1970; Anderson et al., 2003; Lavoie et al., 2013; Ireland et al., 2013).

Householder et al. (2012) argued that the underlying substrate topography of peatlands covering abandoned channels, swales and ridges in Madre de Díos, Peru, likely contributes to spatial variation in vegetation communities. For example, palm forest on deep peat often grades into open swamp on shallow peat. The pollen data from Quistococha show that deeper areas of

the site have been occupied by different vegetation to shallow areas through time, which is consistent with the observation of Householder et al. (2012). For example, shallower areas of peat have a more prominent mixed Arecaceae phase (e.g. QT-2012-10, QT-2012-18). As the basin fills with peat, topographic variations should be largely smoothed out, potentially driving a long-term trend towards greater homogeneity (with a decreasing variety of vegetation assemblages across different parts of the site). This seems to have occurred during Phase IV at Quistococha.

Although there are pronounced similarities in the pollen records from the different peat cores (NMDS biplots (Figure 7) show that all the sequences show a similar change from samples dominated by Cecropiaceae and Cyperaceae, to Myrtaceae-dominated samples, to samples rich in *Mauritia*-t pollen), there are also variations in vegetation communities between cores. These can be seen in the varied trajectories of the NMDS plots. Palynological differences between cores are greater in the lower and middle pollen zones than in the upper-most zones; examples include the peak in Melastomataceae/Combretaceae in QT-2011-2 (Q2-B), and the pronounced peaks in *Euterpe*-t. pollen in QT-2012-10 and QT-2012-18 relative to QT-2010-1 where *Euterpe*-t. pollen remains <10% throughout. Similarly, Myrtaceae pollen remains <5% throughout QT-2012-18, whereas all of the other cores contain a Myrtaceae phase.

The transport distance for the pollen entering the peat cores was likely low except during the initial phases of site development (Phase I & II), where the presence of herbaceous taxa (Poaceae, Cyperaceae) suggests a more open canopy. The lake core (QT-2010-3) contains high percentages of *Cecropia* (15-25%) and Moraceae (15-30%) pollen throughout the last 2500 years, likely representing the abundance of these pollen types in the regional pollen rain (Kelly et al., 2018). The absence of these in similar quantities in the later pollen zones from the peat cores suggests that the canopy was closed at this time, and therefore that the pollen source area for the peat cores was relatively low (10s of metres). Thus, the palynological differences between cores likely reflect genuinely greater spatial heterogeneity in the vegetation during the earlier history of the peatland than in the last 200 years to the present day. This in part reflects the increasing palynological dominance of *Mauritia*-t. at all sites through time. Today, the vegetation across the site is dominated by *M. flexuosa*, *M. armata* and *T. insignis var. monophylla,* and appears in remote sensing imagery to be rather uniform at the 100 m scale across most of the site.

One potential mechanism linking peat depth to vegetation composition is the declining access of plant roots to the nutrient resources of mineral substrate as the peat thickens. This mechanism is used in, for example, the Holocene Peat Model (Frolking et al., 2010) to drive plant succession as the peat accumulates. The contribution of the mineral substrate to peatland nutrient budgets has not been studied in tropical contexts, although geochemical analysis of the sediments at Quistococha has shown that they contain an abundance of essential plant nutrients such as potassium (Lawson et al., 2014). However, even if this substrate nutrient pool is important, peatland hydrology, which controls the flux of nutrients to and within the peatland, is likely to be affected by the subsurface and surface topographies in complex ways that involve feedbacks between the peat and the vegetation operating over multiple temporal and spatial scales. Subsurface flow will be affected by buried features such as the curvilinear ridges typical of fossilized meanders (Kalliola et al., 1991a), and by variations in the hydraulic conductivity of the peat, which in turn is likely to depend on its botanical composition and degree of decomposition (Kelly et al., 2014). The topography of the peat surface may be partly inherited from the substrate, and further modified by (*inter alia*) tree buttresses, coarse litter fall, and tree tip-ups (Dommain et al., 2014). In broad terms, complex surface topography translates to heterogeneity in hydrological and geochemical environments, but it also affects the hydrology of the site as a whole by e.g. reducing the rate of surface runoff. At a finer scale, microtopographic variation, such as the leaf hummocks produced by *Mauritia*, is likely to affect succession in tropical peatlands, just as it does in peatlands elsewhere in the world (e.g. Økland et al., 2008; Harris and Baird, 2019). The significance of these different processes in driving ecological patterning in time and space, and thereby in driving trends in alpha and beta diversity through time, should be a focus for future tropical peatland research.

5.4 Challenges with modelling peat carbon accumulation

The present study has highlighted three specific challenges for the numerical modelling of long-term carbon accumulation rates in Amazonian peatlands:

i) Variation in vegetation types across the site through time means that net primary productivity (NPP), the main input for carbon accumulation equations, may also vary substantially (Lawson et al., 2015). Detailed field measurements from a range of vegetation types will be needed to assess the extent of this variation.

ii) The undulating substrate topography means that modelling water table depth, one of the main factors affecting aerobic respiration rates (and hence peat decay), is more complicated than if the basin had a simpler geometry.

iii) Different parts of the site were subject to varying sediment input, particularly during the early stages of peat accumulation. This has the effect of increasing carbon accumulation rates during the period before pure peat initiation (Lähteenoja et al., 2009) through incorporation and rapid burial of organic matter at low percentages but higher accumulation rates.

The past carbon accumulation of the peatland at Quistococha and four others (San Jorge, Aucayacu, Charo, Riñon) was modelled by Wang et al. (2018) as a means of testing the capacity of peat models to predict future carbon accumulation. Of the five peatlands, the model for Quistococha appears to compare most favourably with the palaeoenvironmental data, with relatively little divergence between modelled and measured soil organic carbon accumulation rates. The other peatlands diverge substantially in the early part of their development (0-500 years after peat initiation), with models generally underestimating carbon accumulation. The divergence between the modelled and the observed carbon accumulation at San Jorge is likely to be explained by the input of sediment in the lower part of the core, which appears to result in a higher C accumulation rate prior to start of pure peat accumulation (see Lähteenoja et al., 2009; Kelly et al., 2016). As such, the data from the present study suggest that the agreement between the modelled and observed carbon accumulation rate at Quistococha may be largely coincidental, as cores taken from across the site have varying peat accumulation rates (Table 3). A similar mis-match to that found for San Jorge may be found for points across Quistococha, such as core QT-2012-9, which also has a thick layer of 'muck' (<65% LOI) underlying the peat above.

The present study illustrates the problem with building one-dimensional models which treat a large peatland, around 500 hectares in area (or larger in many cases), as though it were a single point, with uniform vegetation and hydrology that do not change through time. These assumptions are proved to be incorrect by palaeoecological data which indicate that, for example at San Jorge or Quistococha, a point in the peatland which is occupied by palm swamp vegetation at the present day can easily have been a sedge-fern fen or a seasonally-flooded forest in the past (Kelly et al., 2017b). Such spatial and temporal variation may explain much of the divergence between simulated and observed soil carbon accumulation rates (Wang et al., 2018). Further research on spatio-temporal patterns in Amazonian peatland development will help to quantify the inevitable uncertainties in model outputs, and may provide insights (e.g. identification of common developmental patterns) which help to refine our ability to reconstruct and predict carbon accumulation through numerical modelling.

6. Conclusions

Our multiple-core study from Quistococha indicates that, at this site, the multiple-core approach yields greater certainty over the pattern of vegetation change observed in previous studies, provides considerable additional detail on spatial variations through time, enables us to discriminate between different models of peatland development, and indicates the challenges associated with computer modelling of peat accumulation. Following abandonment of a meander bend by the River Amazon before c. 3500 cal yr BP, clayey silts were deposited across the site by floodwaters presumably originating from the Amazon. Peat began to accumulate at our sampling points across the present-day peatland between 1900-2400 cal yr BP. The vegetation at the site was apparently more heterogeneous during earlier phases (Phase III & IV) of the peatland history than it is today; the modern peatland forest is currently dominated by three tree species. It is however possible that heterogeneity in vegetation across the site may increase again in the future if the site becomes domed, with vegetation zones like those seen at sites such as San Jorge establishing themselves. In contrast to previously published models of tropical peatland development in more geomorphologically stable contexts, our results emphasize the varying influence of the Amazon as a major control on vegetation development and, by extension, carbon storage on this floodplain peatland. We recommend that future palaeoecological studies on PMFB peatlands, and beyond, should take seriously the need for replication and exploit the rich potential of spatially-explicit palaeoecology by using a multiple-core approach. This is particularly so in tropical peatlands, where the forest canopy limits long distance transport of pollen to the core site. There are obvious additional costs in terms of time and money, but these can be mitigated by reducing the sampling resolution or counting fewer pollen grains per sample in secondary sequences. Future work should seek to test whether peatlands elsewhere on tropical floodplains show similar developmental patterns, and should investigate in more detail the interactions between substrate and surface topography, hydrology, geochemistry, and vegetation, in the course of tropical peatland development. Within-site heterogeneity has important implications for modelling future carbon accumulation which cannot be ignored.

Supporting Information

Additional supporting information can be found in the online version of this article.

Data Availability

Datasets related to this article can be found at http://dx.doi.org/10.17632/fw2fn6z25p.1 an open-source online data repository hosted at Mendeley Data (Kelly et al., 2020).

Acknowledgements

We gratefully acknowledge financial support from the Royal Geographical Society, and NERC (grant ref. NE/H011773/1 and a quota PhD studentship), including two radiocarbon allocations (refs. 1612.0312, 1558.0411). We thank the Ministerio de Turismo in Iquitos for giving permission to work at Quistococha; F. Draper for assistance with Landsat imagery, O. Lähteenoja, R. Marchant and D. Galbraith for helpful discussions; the *Instituto de Investigaciones de la Amazonía Peruana* for logistical assistance; O. Clark, E. Honorio Coronado, J. Irarica, R. Jurczyk, E. Shattock, W. Murphy, and H. Vásquez for assistance in the field; and D. Ashley, M. Gilpin, and R. Gasior for technical support. We would also like to thank William Gosling and Ethan Householder for their constructive review comments on the final version of the text.

References

Anderson, R.L., Foster, D.R., and Motzkin, G., 2003. Integrating lateral expansion into models of peatland development in temperate New England. Journal of Ecology, 91, 68-76

Anderson, J.A.R., and Muller, J. 1975. Palynological study of a Holocene peat and a Miocene coal deposit from NW Borneo. Review of Palaeobotany and Palynology, 19, 291–351.

Aniceto K, Moreira-Turcq P, Cordeiro RC, Fraizy P, Quintana I, Turcq B 2014a. Holocene paleohydrology of Quistococha Lake (Peru) in the upper Amazon Basin: Influence on carbon accumulation. Palaeogeography Palaeoclimatology Palaeoecology 415, 165–174.

Aniceto K, Moreira-Turcq P, Cordeiro R.C, Quintana I, Fraizy P, Turcq B., 2014b. Hydrological changes in west Amazonia over the past 6 ka inferred from geochemical proxies in the sediment record of a floodplain lake. Procedia Earth and Planetary Science 10, 287–291.

Absy M.L., 1979. *A Palynological Study of Holocene Sediments in the Amazon Basin*. Unpublished PhD Thesis, University of Amsterdam.

Baird, A.J., Morris, P.J., and Belyea, L.R., 2012. The DigiBog peatland development model 1: rationale, conceptual model, and hydrological basis. Ecohydrology 5, 242-255. DOI: 10.1002/eco.230

Bauer, I.E., Gignac, L.D., and Vitt, D.H., 2003. Development of a peatland complex in boreal western Canada: lateral site expansion and local variability in vegetation succession and long-term peat accumulation. Canadian Journal of Botany, 81, 833-847.

Bawa, K.S., Bullock, S.H., Perry, D.R., Coville, R.E., and Grayum, M.H. 1985. Reproductive Biology of Tropical Lowland Rain Forest Trees. II. Pollination Systems. American Journal of Botany, 72, 346-356.

Bhomia, R.K., van Lent, J., Grandez Rios, J.M., Hergoualc'h, K., Honorio Coronado, E.N., and Murdiyarso, D. 2018. Impacts of Mauritia flexuosa degradation on the carbon stocks of freshwater peatlands in the Pastaza-Marañón river basin of the Peruvian Amazon. Mitigation and Adaptation Strategies for Global Change. doi: 10.1007/s11027-018-9809-9

Blaauw, M. 2010. Methods and code for 'classical' age-modelling of radiocarbon sequences. Quaternary Geochronology 5, 512–518.

Bronk Ramsey. 1995. Radiocarbon calibration and analysis of stratigraphy: The OXCAL program. Radiocarbon 37: 425-430.

Bronk Ramsey, C., and Lee, S. 2013. Recent and planned developments of the program OXCAL. Radiocarbon 55, 720-730.

Bunting, M.J., 2003. Pollen–vegetation relationships in non-arboreal moorland taxa. Review of Palaeobotany and Palynology, 125(3), 285–298.

Burn M.J., Mayle F.E., 2008. Palynological differentiation between genera of the Moraceae family and implications for Amazonian palaeoecology. Review of Palaeobotany and Palynology 149, 187–201.

Bush, M.B., Weng, M.B., 2006. Introducing a new (freeware) tool for palynology. J. Biogeogr. 34, 377–380.

Bush, M.B., and Rivera, R., 1998. Pollen dispersal and representation in a neotropical rain forest. Global Ecology and Biogeography Letters, 7, 379–392

Bush, M.B., and Rivera, R., 2001. Reproductive ecology and pollen representation among neotropical trees. Global Ecology and Biogeography 10, 359–367

730 Campbell, D.G., Stone, J.L., and Rosas, A., 1992. A comparison of the phytosociology and
731 dynamics of three floodplain (*Várzea*) forests of known ages, Rio Jurua, western Brazilian
732 Amazon. Botanical Journal of the Linnean Society, 108, 213-237

733 Colinvaux P, De Oliveira P.E, and Moreno J.E., 1999. Amazon Pollen Manual and Atlas.
734 Harwood, Amsterdam.

735 Comas X, Slater, L., and Reeve, A., 2004. Geophysical evidence for peat basin morphology
736 and stratigraphic controls on vegetation observed in a Northern Peatland. Journal of Hydrology,
737 295, 173–184

738 Dias Saba, M., 2007. Morfologia Polínica de Malvaceae: Implicações Taxonômicas e
739 Filogeneticas. Unpublished PhD thesis, Universidade stadual de Feira de Santana.

740 Dommain, R., Cobb, A.R., Joosten, H., Glaser, P.H., Chua, A.F.L., Gandois, L., Kai, F-M.,
741 Noren, A., Salim, K.A., Su'ut, N.S.H., Harvey, C.F., 2015. Forest dynamics and tip-up pools
742 drive pulses of high carbon accumulation rates in a tropical peat dome in Borneo (Southeast
743 Asia). Geophys. Res.-Biogeo. 120, 617–640.

744 Draper, F.C., 2015. Carbon Storage and Floristic Dynamics in Amazonian Peatland
745 Ecosystems. PhD thesis, University of Leeds, U.K.

746 Draper, F.C.H., Roucoux, K.H., Lawson, I.T., Mitchard, E.T.A., Honorio Coronado, E.N.,
747 Lähteenoja, O., Montenegro, L.T., Valderrama Sandoval, E., Zaráte, R., Baker, T.R., 2014.
748 The distribution and amount of carbon in the largest peatland complex in Amazonia. Environ.
749 Res. Lett. 9, 124017.

750 Draper, F.C., Honorio Coronado, E.N.H., Roucoux, K.H., Lawson, I.T., Pitman, N.C.A., Fine,
751 P.V.A., Phillips, O.L., Torres Montenegro, L.A., Valderama Sandoval, E., Mesones, I., Garcia-
752 Villacorta, R., Ramirez Arévalo, F.R., and Baker, T.R., 2017. Peatland forests are the least
753 diverse tree communities documented in Amazonia, but contribute to high regional beta-
754 diversity. Ecography 14, 1256-1269. DOI: 10.1111/ecog.03126

755 Endress, B.A., Horn, C.A., & Gilmore, M.P., 2013. *Mauritia flexuosa* palm swamps:
756 Composition, structure and implications for conservation and management. Forest Ecology and
757 Management, 302, 346–353.

758 Faegri, K. and Iverson, J., 1989. Textbook of pollen analysis. John Wiley: Chichester, UK

759 Frolking, S., Roulet, N.T., Tuittila, E., Bubier, J.L., Quillet, A., Talbot, J., & Richards, P.J.H.,
760 2010. A new model of Holocene peatland net primary production, decomposition, water
761 balance, and peat accumulation. Earth System Dynamics, 1, 1-21

762 Gentry, A.H., 1993. A Field Guide to the Families and Genera of Woody Plants of Northwest
763 South America (Colombia, Ecuador, Peru) with Supplementary Notes on Herbaceous Taxa.
764 Conservation International, Washington D.C., U.S.A.

765 Gosling, W.D., Mayle, F.E., Tate, N.J., Killeen, T.J., 2009. Differentiation between
766 Neotropical rainforest dry forest and savannah ecosystems by their modern pollen spectra and
767 implications for the fossil pollen record. Rev. Palaeobot. Palyno. 153, 70–85.

768 Harris, A., Baird, A.J., 2019. Microtopographic Drivers of Vegetation Patterning in Blanket
769 Peatlands Recovering from Erosion. Ecosystems 22, 1035–1054

770 Heinselman, M.L., 1963. Forest Sites, Bog Processes, and Peatland Types in the Glacial Lake
771 Agassiz Region, Minnesota. Ecological Monographs 33, 327–374.

772 Hiraoka, M., 1999. Miriti (Mauritia flexuosa) Palms and Their Uses and Management among
773 the Ribeirinhos of the Amazon Estuary. Advances in Economic Botany 13, 169-186.

774 Honorio Coronado, E.N., Vega Arenas, J.E., and Corrales Medina, M.N., 2015. Diversidad,
775 estructura y carbon de los bosques aluviales del Noreste Peruano. Folia Amazonica**,** 24, 55–70

776 Householder, J.E., Janovec, J.P., Tobler, M.W., Page, S., Lähteenoja, O., 2012. Peatlands of
777 the Madre de Dios river of Peru: distribution, geomorphology, and habitat diversity. Wetlands
778 32, 359–368.

779 Huisman, S.N., Raczka, M.F., McMichael, C.N.H. 2018. Palm Phytoliths of Mid-Elevation
780 Andean Forests. Frontiers in Ecology and Evolution 6, 193. doi: 10.3389/fevo.2018.00193

781 Ireland, A.W., and Booth, R.K., 2011. Hydroclimatic variability drives episodic expansion of
782 a floating peat mat in a North American kettlehole basin. Ecology, 92, 11-18.

783 Ireland, A.W., Booth, R.K., Hotchkiss, S.C., and Schmitz, J.E., 2012. Drought as a Trigger for
784 Rapid State Shifts in Kettle Ecosystems: Implications for Ecosystem Responses to Climate
785 Change. Wetlands, 32, 989-1000.

786 Ireland, A.W., Booth, R.K., Hotchkiss, S.C., and Schmitz, J.E., 2013. A comparative study of
787 within-basin and regional peatland development: implications for peatland carbon dynamics.
788 Quaternary Science Reviews, 61, 85-95.

789 Jacobson, G.L., and Bradshaw, R.H.W., 1981. The selection of sites for paleovegetational
790 studies. Quaternary Research, 16, 80-96

791 Jowsey P.C., 1966. An improved peat sampler. New Phytologist 65, 245–248.

792 Kalliola, R., Salo, J., Puhakka, M., Marjut, R., 1991a. New site formation and colonizing
793 vegetation in primary succession on the Western Amazon floodplains. J. Ecol. 79, 877–901.

794 Kalliola, R., Puhakka, M., Salo, J., Tuomisto, H., & Ruokolainen, K. 1991b. The dynamics,
795 distribution and classification of swamp vegetation in Peruvian Amazonia. Ann. Bot. Fennici
796 28, 225–239.

797 Kelly, T.J., Lawson, I.T., Roucoux K.H, Baker, T.R., Jones, T.D., Honorio Coronado, E.N., &
798 Rivas Panduro, S., 2018. Continuous human presence without extensive ecological disturbance
799 over the past 2500 years in an aseasonal Amazonian rainforest. Journal of Quaternary Science
800 DOI: 10.1002/jqs.3019/full

801 Kelly, T.J., Baird, A.J., Roucoux, K.H., Baker, T.R., Honorio Coronado, E.N., Ríos, M.,
802 Lawson, I.T., 2014. The high hydraulic conductivity of three wooded tropical peat swamps in
803 northeast Peru: measurements and implications for hydrological function. Hydrol. Process. 28,
804 3373–3387.

805 Kelly, T.J., Cole, L.S.E., & Lawson, I.T., 2017a. Peat. In: White, W. (ed.) Encyclopedia of
806 Geochemistry. Springer International: Switzerland

807 Kelly T.J., Lawson I.T., Roucoux K.H., Baker T.R., Jones T.D., Sanderson N.K., 2017b. The
808 vegetation history of an Amazonian domed peatland. Palaeogeography, Palaeoclimatology,
809 Palaeoecology 468, 129–141.

810 Kelly, T.J., 2015. The long-term development of peatlands in the Peruvian Amazon. PhD
811 thesis, University of Leeds, U.K.

812 Kvist, L.P., and Nebel, G., 2001. A review of Peruvian flood plain forests: ecosystems,
813 inhabitants and resource use. Forest Ecology and Management, 150, 3-26

814 Lähteenoja, O., Page, S., 2011. High diversity of tropical peatland ecosystem types in the
815 Pastaza-Marañón basin, Peruvian Amazonia. J. Geophys. Res. 116, G02025.

816 Lähteenoja, O., Reátegui, Y.R., Räsänen, M., Torres, D.D., Oinonen, M., Page, S., 2012. The
817 large Amazonian peatland carbon sink in the subsiding Pastaza-Marañón foreland basin, Peru.
818 Glob. Change Biol. 18, 164–178.

819 Lähteenoja, O., Flores, B., and Nelson, B., 2013. Tropical Peat Accumulation in Central
820 Amazonia. Wetlands, 33, 495-503.

821 Lähteenoja, O., Ruokolainen, K., Schulman, L., and Oinonen, M., 2009a. Amazonian
822 peatlands: an ignored C sink and potential source. Global Change Biology, 15, 2311–2320.

823 Lähteenoja, O., Ruokolainen, K., Schulman, L., and Alvarez, J., 2009b. Amazonian floodplains
824 harbour minerotrophic and ombrotrophic peatlands. Catena, 79, 140–145.

825 Lavoie, M., Pellerin, S., Larocque, M., 2013. Examining the role of allogenous and autogenous
826 factors in the long-term dynamics of a temperate headwater peatland (southern Québec,
827 Canada). Palaeogeography, Palaeoclimatology, Palaeoecology 386, 336-348

828 Lawson I.T, Jones T.D, Kelly T.J., Honorio Coronado E.N., Roucoux K.H., 2014. The
829 geochemistry of Amazonian peats. Wetlands 34, 905–915.

830 Mertes, L.A., 1997. Documentation and significance of the perirheic zone on inundated
831 floodplains. Water Resour. Res. 33, 1749–1762.

832 Nowicke, J.W., Takahashi, M. (2002) Pollen morphology, exine structure and systematics of
833 Acalyphoideae (Euphorbiaceae), Part 4: Tribes Acalypheae pro parte (Erythrococca,
834 Claoxylon, Claoxylopsis, Mareya, Mareyopsis, Discoclaoxylon, Micrococca, Amyrea,
835 Lobanilia, Mallotus, Deuteromallotus, Cordemoya, Cococceras, Trewia, Neotrewia,
836 Rockinghamia, Octospermum, Acalypha, Lasiococca, Spathiostemon, Homonoia),
837 Plukenetieae (Haematostemon, Astrococcus, Angostyles, Romanoa, Eleutherostigma,
838 Plukenetia, Vigia, Cnesmone, Megistostigma, Sphaerostylis, Tragiella, Platygyna, Tragia,
839 Acidoton, Pachystylidium, Dalechampia), Omphaleae (Omphalea), and discussion and
840 summary of the complete subfamily. Rev. Palaeobot. Palyno. 121, 231–336.

841 Økland, R.H., Rydgren, K., and Økland, T., 2008. Species richness in boreal swamp forests
842 of SE Norway: The role of surface microtopography. Journal of Vegetation Science 19, 67-74
843
844 Oksanen, J, Blanchet, F.G., Kindt, R., Legendre, P., Minchin, P.R., O'Hara, R.B., Simpson,
845 G.L., Solymos, P., Stevens, M.H.H., and Wagner, H. 2015. vegan: Community Ecology
846 Package. R package version 2.3-2. http://CRAN.R-project.org/package=vegan

847 Page, S.E., Rieley, J.O., Banks, C.J., 2011. Global and regional importance of the tropical
848 peatland carbon pool. Glob. Change Biol. 17, 798–818.

849 Parodi, J.L., and Freitas, D. 1990. Geographical aspects of forested wetlands in the Lower
850 Ucayali, Peruvian Amazonia. Forest Ecology and Management, 33/34, 157-168

851 Patterson, T, Huckerby, G., Kelly, T.J., Swindles, G.T., Nasser, N.A., 2015. Hydroecology of
852 Amazonian lacustrine Arcellacea (testate lobose amoebae): a case study from Lake
853 Quistococha, Peru. Eur. J. Protistol. 51, 460–469.

854 Phillips, S., Rouse, G.E., Bustin, R.M., 1997. Vegetation zones and diagnostic pollen profiles
855 of a coastal peat swamp, Bocas del Torro, Panamá. Palaeoegeography, Palaeoclimatology,
856 Palaeoecology, 128, 301-338.

857 R Core Team, 2014. R: A language and environment for statistical computing. R Foundation
858 for Statistical Computing, Vienna, Austria. URL http://www.R-project.org/.

859 Räsänen, M., Neller, R., Salo, J., Jungner, H., 1992. Recent and ancient fluvial deposition
860 systems in the Amazon foreland basin, Peru. Geol. Mag. 129, 293–306.

861 Reimer, P.J., Bard, E., Bayliss, A., Beck, J.W., Blackwell, P.G., Bronk Ramsey, C., Buck, C.E.,
862 Edwards, R.L., Friedrich, M., Grootes, P.M., Guilderson, T.P., Haflidason, H., Hajdas, I.,
863 Hatté, C., Heaton, T.J., Hoffman, D.L., Hogg, A.G., Hughen, K.A., Kaiser, K.F., Kromer, B.,
864 Manning, S.W., Niu, M., Reimer, R.W., Richards, D.A., Scott, M., Southon, J.R., Staff, R.A.,
865 Turney, C.S.M., and van der Plicht, J. 2013. IntCal13 and Marine13 radiocarbon age calibration
866 curves 0–50,000 years cal BP. Radiocarbon, 55: 1869-1887

867 Rivas Panduro S, Panaifo Texeira M, Oyuela-Caycedo A, Zimmerman A., 2006. Informe
868 preliminar sobre los hallazgos en el sitio archeológico de Quistococha, Amazonía peruana.
869 Boletin de Estudios Amazonicos 1, 79–98.

870 Roberts, D.W., 2016. labdsv: Ordination and Multivariate Analysis for Ecology. R package
871 version 1.8-0. http://CRAN.R-project.org/package=labdsv

872 Roubik D.W, Moreno J.E., 1991. Pollen and Spores of Barro Colorado Island. Missouri
873 Botanical Garden, St Louis.

874 Roucoux K.H, Lawson I.T, Jones T.D, Baker T.R, Coronado E.N, Gosling W.D, Lähteenoja
875 O., 2013. Vegetation development in an Amazonian peatland. Palaeogeography,
876 Palaeoclimatology, Palaeoecology 374, 242–255.

877 Roucoux, K.H., Lawson, I.T., Baker, T.R. Del Castillo Torres, D., Draper, F.C., Lahteenoja,
878 O., Gilmore, M., Honorio Coronado, E.N., Kelly, T.J., Mitchard, E.T.A., and Vriesendorp, C.

879 2017. Threats to Amazonian peatlands and opportunities for their conservation. Conservation
880 Biology DOI: 10.1111/cobi.12925

881 Seubert, E., 1996. Root anatomy of palms II: Calamoideae. *Feddes Repertorium*, 107: 43-59

882 Sjörs, H., 1983. Mires of Sweden. In: Gore, A.J.P. (ed.) Ecosystems of the world. 4B. Mires:
883 swamp, bog, fen and moor. Elsevier: Amsterdam, 69-94.

884 Stockmarr, J. 1971. Tablets with spores used in absolute pollen analysis. *Pollen et Spores*, 13:
885 615-621.

886 Swindles, G.T., Kelly, T.J., Roucoux, K.H., and Lawson, I.T. (2018) Response of testate
887 amoebae to a late Holocene ecosystem shift in an Amazonian peatland. European Journal of
888 Protistology 64, 13-19

889 Tansley, A.G., 1935. The use and abuse of vegetational concepts and terms. Ecology, 16, 284-
890 307.

891 Teh Y.A., Murphy W.A., Berrio J-C, Boom A, Page S.E., 2017. Seasonal variability in methane
892 and nitrous oxide fluxes from tropical peatlands in the western Amazon basin. Biogeosciences
893 14, 3669–3683.

894 Van Geel, B., 2001. Non-pollen palynomorphs. In: Smol, J.P., Birks, H.J.B., Last, W.M.,
895 (Eds.), Tracking Environmental Change Using Lake Sediments. Volume 3: Terrestrial, Algal,
896 and Siliceous indicators. Kluwer, Dordrecht, The Netherlands, pp. 99–119.

897 Walker, D., 1970. Direction and rate in some British post-glacial hydroseres. In: Walker, D.
898 and West, R.G. (eds) *Studies in the Vegetational History of the British Isles*. Cambridge
899 University Press: Cambridge, 117-139

900 Walker J.W., Walker A.G., 1979. Comparative pollen morphology of the American
901 Myristicaceous genera Campsoneura and Virola. Annals of the Missouri Botanic Garden 66,
902 731–755.

903 Wang, S., Zhuang, Q., Lahteenoja, O., Draper, F.C., Cadillo-Quiroz, H., 2018. Potential shift
904 from a carbon sink to a source in Amazonian peatlands under a changing climate. Proceedings
905 of the National Academy of Sciences, 115 (49), 12407-12412

906 Weber, M., Halbritter, H., and Hesse, M., 1999. The Basic Pollen Wall Types in Araceae.
907 International Journal of Plant Sciences, 160, 415-423

908 Wittman, F., Schöngart, J., Montero, J.C., Motzer, T., Junk, W.J., Piedade, M.T.F., Queiroz,
909 H.L., and Worbes, M., 2006. Tree species composition and diversity gradients in white-water
910 forests across the Amazon Basin. Journal of Biogeography, 33, 1334-1347

911 Wüst, R.A., Bustin, R.M., and Lavkulich, L.M., 2003. New classification systems for tropical
912 organic-rich deposits based on studies of the Tasek Bera Basin, Malaysia. Catena, 53, 133-163

913

914

915 ## Tables

916 **Table 1:** Key details of the developmental phases reconstructed for the Quistococha lake and
917 peatland from the six palaeoecological records for the site and the basal dates on six other cores.
918 Chr. = the basis for the chronology of each phase (symbols given beneath table). Pollen zones
919 with a 'QT1' prefix refer to Roucoux et al. (2013). In contrast to normal geological convention,
920 the oldest phase is given at the top.

Phase	Summary	Timing
I. Amazon floodplain	The Quistococha basin was abandoned as an active meander of the Amazon sometime before 4500 cal yr BP, but regular flooding by the Amazon continued to dominate deposition until c. 2400 cal yr BP. **Indicator taxa**: *Cecropia*, Cyperaceae Pollen zones: Q9-A, QT1-A (Q3-A in lake core).	4,500–-2,400 cal yr BP **Chr.:** R, L
II. Herbaceous sedge fen	Peat initiated in the area within 800 m of the lake aided by the impermeable clay substrate. Pollen evidence indicates largely herbaceous vegetation with abundant Cyperaceae at this time. Some cores contain pollen which suggests the presence of taller trees (e.g. Anacardiaceae in QT-2011-2). The peatland expanded to cover the southern part of the site through 'primary mire formation' as the influence of the river declined. *Symmeria paniculata*, a small tree tolerant of deep flooding, was prevalent across large parts of the site. **Indicator taxa:** *Symmeria paniculata*, *Adelobotrys*-t., *Begonia*, *Cecropia*, Cyperaceae*, Brosimum*, Moraceae, *Maquira*-t. **Pollen zones:** Q2-A, Q9-B, Q10-A, Q18-A, QT1-B, QT-3	1,900–2,400 cal yr BP **Chr.:** P, R
III. Mixed angiosperm flooded forest	The site continued to be flooded annually, as indicated by the presence of Myrtaceae. Shrubby taxa were prevalent across the site, especially Rubiaceae types such as *Psychotria*. Increase of *Mauritia*-t. in the lake core is interpreted as the result of *Mauritia* stands along the western lake margin. **Indicator taxa:** Myrtaceae, *Coussapoa*, Rubiaceae, Rubiaceae (type 2), Mel./Comb., *Adelobotrys*-t., *Psychotria*-t., *Brosimum*. **Pollen zones:** Q2-B, Q9-C, Q10-A, Q18-B, QT1-C, QT1-D	1,900–1,100 cal yr BP [remnant around the lake until 566-678 cal yr BP] **Chr.:** P, R

IV. Mixed palm swamp	*Euterpe*-t. pollen phases are seen across the site, particularly in shallow peat areas (e.g. QT-2012-10, QT-2012-18). *Mauritia* and *Mauritiella* are both abundant across the site, especially in deeper peat areas (e.g. QT-2010-1). A second expansion of mixed palm swamp along the eastern lake margin was related to the delayed terrestrialisation of this area, and it is inferred that Myrtaceae and other flood tolerant taxa also lingered until this transition (Myrtaceae, although low in abundance, declines in the lake core c. 650 cal yr BP). **Indicator taxa:** *Euterpe*-t., *Symphonia globulifera*, *Alchornea*, *Ilex*. **Pollen zones:** Q2-C, Q9-D & Q9-E, Q10-C, Q18-C, QT1-E	1,100–400 cal yr BP [second expansion: 566-678 cal yr BP] **Chr.:** P, R
V. Mauritia-dominated palm swamp	The site approached its present day form, with *Mauritia* and *Mauritiella* both very abundant. *Tabebuia* is found during Phase IV, but becomes more abundant in some cores during Phase V. There is less variation in the vegetation between shallow and deep peat areas. **Indicator taxa:** *Mauritia*-t., *Tabebuia*-t., Bombacaceae. **Pollen zones:** Q2-D, Q9-E, Q10-D, Q18-D, QT1-F	400 cal yr BP – present **Chr.:** R, L

L: Lake core R: QT-2010-1 (Roucoux et al., 2013) P: Peat cores, this study

921

Table 2: Radiocarbon age determinations for Quistococha peat cores. AMS radiocarbon dates were obtained from the NERC facility at East Kilbride. Calibration was undertaken using the INTCAL13 curve. All samples are the < 180 μm peat fraction. (*Sample inferred to have been affected by young carbon contamination from root penetration.) Four dates were targeted specifically at dating the main increase in *Mauritia*-t. pollen, and three at the lower peak in *Mauritia*-t (marked *ψ*) seen in some of the cores studied (see Figure 4).

Core	Laboratory code	Depth (cm)	^{14}C age (yrs BP)	s.d.	δ^{13}C	Calibrated age (cal yr BP)
Peat basal dates						
QT-2011-1*	SUERC-44988	130	859	37	-30.3	709-891
QT-2011-2 *ψ*	SUERC-44989	196	2155	35	-30.1	2067-2301
QT-2011-3	SUERC-44990	178	2234	37	-16.1	2159-2325
QT-2011-4	SUERC-44991	352	2253	35	-29.8	2181-2337
QT-2011-5	SUERC-44992	226	1988	37	-30.7	1897-1987
QT-2011-6	SUERC-44995	320	2061	37	-30.2	1953-2109
QT-2011-7	SUERC-44996	262	2228	35	-29.7	2159-2315
QT-2012-9	SUERC-54428	256	2,324	41	-29.6	2209-2315
QT-2012-10 *ψ*	SUERC-54429	180	2,290	41	-30.8	2186-2352
QT-2012-18	SUERC-54432	144	2,059	41	-30.3	1952-2111
Main* Mauritia-t. *increase						
QT-2011-2	SUERC-54423	130	1,164	40	-30.0	1008-1174
QT-2012-9	SUERC-54424	96	684	39	-30.1	566-676
QT-2012-10	SUERC-54425	112	1,144	40	-31.2	978-1172
QT-2012-18	SUERC-54426	96	1,030	41	-30.7	916-980
Lower* Mauritia-t. *peak (also Ψ above)						
QT-2012-9	SUERC-54427	192	1,771	41	-29.5	1615-1733

Table 3: Peat accumulation rates derived from peat basal dates

	Peat accumulation rate (mm/yr)	
Core	**Maximum**	**Minimum**
QT-2011-1	1.69	1.37
QT-2011-2	0.92	0.83
QT-2011-3	0.80	0.75
QT-2011-4	1.57	1.47
QT-2011-5	1.15	1.10
QT-2011-6	1.59	1.47
QT-2011-7	1.18	1.10
QT-2012-9	1.13	1.08
QT-2012-10	0.80	0.75
QT-2012-18	0.71	0.66
Average	1.15	1.06
Standard deviation	0.357	0.306

933 **Table 4:** Pollen assemblage zone summary descriptions for QT-2011-2. A summary of the
934 palm phytolith data has also been provided. Zones have been shown in stratigraphic order (i.e.
935 the uppermost pollen zone is at the top of the table). A summary of the palm phytolith data has
936 also been provided. Indications of abundance refer to the maximum phytolith concentrations
937 in a given zone, where 'extremely abundant' corresponds to >200,000 phytoliths cm^{-3},
938 'present' corresponds to >5,000 phytoliths cm^{-3}, and 'rare' corresponds to < 1,000 phytoliths
939 cm^{-3}. Phytoliths were not recorded in the basal zone due to HF treatment.

940

Zone (depths)	Pollen assemblage zone characteristics
Q2-D (91-16 cm)	*Mauritia* t. peaks in this zone (79%) and is the dominant taxon. *Alchornea* sp. declines to ≤ 10% from its peak values in the zone below. Amongst the minor taxa, *Amanoa* sp. peaks in this zone (4%). *Tabebuia* t. is consistently present, but remains uncommon (max. 2%). **Spores:** *Nephrolepis* sp. is abundant and increases towards to the top of this zone where it peaks at 70%. **Palm phytoliths**: extremely abundant
Q2-C (138-91 cm)	*Euterpe* t. increases to its peak at the base of the zone (20%) before declining to 10% at the top of the zone. *Mauritia* t. exceeds 25%. Amongst the minor types, *Symphonia globulifera* is consistently present. Moraceae undiff declines to ≤ 5% from its peak in the zone below. **Spores:** *Selaginella* sp. peaks in this zone 8%. **Palm phytoliths:** extremely abundant
Q2-B (220-138 cm)	Dalbergia/Machaerium t. (12%), Melastomataceae/Combretaceae undiff (30%), Moraceae undiff. (11%), Myrtaceae undiff (10%), Psychotria t. (14%), and Rubiaceae Type I-34 (8%) all peak in this zone. *Mauritia* t. pollen exceeds 5% for the first time (10%). Amongst the rare types, *Alibertia* t. peaks at the base of this zone (5%). *Ilex* sp. and *Macrolobium* sp. also peak in this zone but do not exceed 5%. **Spores:** Monolete fern spores peak in this zone (25%). Algal spores are present in low numbers towards the base of the zone. **Palm phytoliths**: present
Q2-A (232-220 cm)	*Symmeria paniculata* (44%), Ficus sp. (15%), Cyperaceae (11%), and Anacardiaceae (36%) all peak in this zone. *Cecropia* sp. increases from 2% to 18% at the top of this zone. **Spores:** Fern spores are all low in abundance (< 6%). **Palm phytoliths:** all samples in zone HF treated

941

942 **Table 5:** Pollen assemblage zone summary descriptions for QT-2012-9. A summary of the
943 palm phytolith data has also been provided (see caption for Table 4).

Zone (depths)	Pollen assemblage zone characteristics

Q9-E (16-104 cm)	*Mauritia* t. expands from 5% in the zone below to its peak of 63% at 32 cm. *Euterpe* t. peaks at the base of this zone (13%) before declining to < 1% towards the surface. *Alchornea* sp. is also abundant and peaks at 64 cm (15%). *Luehea* t. (max. 6%) and Type Z-9 (max. 10%) also peak in the lower part of this zone. *Ficus* sp. is abundant in the lowermost sample in this zone (max. 16%) but declines to less than 1% at 16 cm. **Spores:** *Nephrolepis* sp. expands markedly towards the top of this zone (max. 43%). *Selaginella* sp. peaks towards the base of this zone (23%). **Palm phytoliths:** extremely abundant
Q9-D (104-120 cm)	This zone consists of a single sample and is characterised by a peak in *Ficus* sp. (70%). *Mauritia* t. is also present but in relatively low proportions (< 10%), and *Euterpe* t. is also present (max. 9%). **Palm phytoliths:** present
Q9-C (120-232 cm)	Myrtaceae has two definable peaks in this zone at 224 cm (28%) and 144 cm (15%). Several Rubiaceae types are moderately abundant in this zone; *Psychotria* t. peaks at 144 cm (13%), *Sabicea* t. peaks at 224 cm (16%), and Type I-34 peaks at 128 cm (16%). Cyperaceae is present but generally remains below 10%, except for a peak at 160 cm (53%). Poaceae remains moderately abundant (max. 8%). *Alchornea* sp. is consistently present (5-10%). Amongst the minor taxa, Malpighiaceae (5%) and *Pouzolzia* t. (5%) both peak in this zone. *Pistia stratiotes* is most common in this zone but does not exceed 10%. **Spores:** Both monolete spores and *Nephrolepis* sp. peak in this zone (70% and 64% respectively). **Palm phytoliths:** present
Q9-B (232-340)	Cyperaceae peaks in this zone and exceeds 10% throughout, but its abundance is variable (10-57%). Poaceae is also moderately abundant and peaks in this zone (17%). *Alibertia* t. is generally low in abundance but peaks in this zone (11%). Amongst the minor types, *Mimosa* sp. is present in low number (max 4.5%) towards the top of this zone. **Spores:** The fern *Pityrogramma* sp. peaks and is consistently present. Algal spores remain abundant throughout the lower half of this zone. **Palm phytoliths:** present
Q9-A (340-344)	This zone consists of a single sample and is dominated by the pollen of *Cecropia* sp., which peaks in this zone (91%). Poaceae, Asteraceae, Cyperaceae and *Alchornea* sp. are all present but in low abundance (< 5%). **Spores:** Algal spores are most abundant in this zone. **Palm phytoliths:** Sample HF treated (no data)

944

945 **Table 6:** Pollen assemblage zone summary descriptions for QT-2012-10. A summary of the
946 palm phytolith data has also been provided (see caption for Table 4).

947

Zone (depths)	Pollen assemblage zone characteristics
Q10-D (16-72 cm)	*Mauritia* t. peaks in this zone (77%) and is the dominant taxon. *Cecropia* sp. and *Alchornea* sp. are moderately abundant throughout, but do not exceed 10% and 13% respectively. *Euterpe* t. declines from its peak in the zone below to < 5%. Amongst the rare types, *Tabebuia* t. is consistently present and peaks at the top of this zone (5%). **Spores:** Trilete spores are abundant throughout and reach their peak of 12%. **Palm phytoliths**: extremely abundant
Q10-C (72-120 cm)	*Euterpe* t. increases from 26% to its peak (63%) at the top of this zone and is the dominant taxon. *Mauritia* t. exceeds 25% for the first time (max. 41%). *Luehea* t. peaks at 7%, and and there is also a peak in Type Z-9 (24%). **Palm phytoliths:** extremely abundant

Q10-B (120-136 cm)	This zone consists of a single sample and is marked by the high abundance of *Cecropia* sp., which peaks in this zone (64%). *Psychotria* t. peaks in this zone (6%), and Type I-34 (max. 7%) is also moderately abundant. Amongst the minor taxa, Myrtaceae (max. 2%) and Asteraceae (max. 3%) are also present. **Palm phytoliths:** present
Q10-A (136-192 cm)	Myrtaceae increases from < 5% to its peak of 20%. *Alchornea* sp. peaks in this zone (14%) and *Psychotria* type is also moderately abundant (6%). *Cecropia* sp. is fairly abundant towards the base of this zone (max. 18%). There is a small peak in *Mauritia* t. at 176 cm (14%). There are also a number of peaks amongst the rarer taxa, such as *Pouzolzia* t. (7%), *Symmeria paniculata* (7%), Asteraceae (6%), and Adelobotrys sp. (4%). *Brosimum* sp. and *Ficus* sp. are consistently present but remain ≤ 6% and ≤ 3% respectively. **Spores:** Algal spores are low in abundance but consistently present throughout this zone. **Palm phytoliths:** present (note: basal sample HF treated)

Table 7: Pollen assemblage zone descriptions for QT-2012-18. Pollen assemblage zone summary descriptions for QT-2012-10. A summary of the palm phytolith data has also been provided (see caption for Table 4). Phytoliths were not recorded in the basal zone due to HF treatment.

Zone (depths)	Pollen assemblage zone characteristics
Q18-D (56-16 cm)	*Mauritia* t. peaks in the top two samples of this zone (70%), but *Euterpe* t. pollen declines from its high values in the zone below to < 3%. Both *Alchornea* sp. and *Cecropia* sp. remain present but do not exceed 10%. Amongst the more minor taxa both *Amanoa* sp. (4%) and *Tabebuia* t. (3%) attain their peak abundance. **Spores:** Trilete spores peak in this zone (8%). **Palm phytoliths:** extremely abundant
Q18-C (104-56 cm)	*Euterpe* t. peaks in this zone, and *Mauritia* t. exceeds 25% for the first time (max. 55%). *Alchornea* sp. also peaks at the top of this zone (19%). Amongst the minor taxa, *Ficus* sp. exceeds 1% throughout. *Cecropia* sp. attains its lowest value in the whole of the core at the base of this zone. **Palm phytoliths:** extremely abundant
Q18-B (140-104 cm)	Poaceae (18%), *Psychotria* t. (23%), Dalbergia/Machaerium t. (8%), small < 12 um Solanaceae (24%) and Solanaceae undiff (30%) all peak within this zone. Cyperaceae is present but declines from its peak in the zone below and remains < 5%. *Adelobotrys* sp. also declines from its peak in the zone below but remains abundant (max. 10%). Amongst the minor types, this zone sees a peak in *Macrolobium* sp. (3%). **Palm phytoliths:** present
Q18-A (160-140 cm)	*Symmeria paniculata* peaks at the base of this zone (35 %), and is consistently abundant throughout (> 10 %). *Adelobotrys* (18%), *Cecropia* sp. (10%), *Ficus* sp. (7%) And Cyperaceae (9%) also peak in this zone. *Mauritia* t. and *Euterpe* t. pollen are present but remain low in abundance. Poaceae is consistently present but remains < 5%. Amongst the minor types, *Bactris* aff. *riparia* (3%), *Begonia* sp. (2%), and Asteraceae (3%) all peak in this zone. **Spores:** The ferns *Nephrolepis* sp. and *Polypodium* t. are most abundant in this zone but both remain < 5%. Algal spores are most abundant in this pollen zone. **Palm phytoliths:** all samples in zone HF treated

Figure captions

Figure 1: Location of sites discussed in the text. (a) Location of the the Pastaza Maranon Foreland Basin in South America. (b) False-colour Landsat TM image indicating the location of the two lowland Amazonian peatland sites mentioned in the text, Quistococha (Roucoux et al., 2013; present study) and San Jorge (Kelly et al., 2016). The town of Tamshiyacu and city of Iquitos (filled circles) are shown for reference. (c) Inferred Quistococha peatland margins based on Landsat imagery and field observations (dashed line). Dark grey shading shows land over 100 m above sea level, and light grey shading shows the floodplain (elevation c. 90m) inferred from Shuttle Radar Topography Mission (SRTM) data (http://srtm.csi.cgiar.org).

Figure 2: Core transects indicating peat depth for the peatland at Quistococha. Core points are shown with arrows and those points selected for pollen analysis are labelled. The peatland is underlain by minerogenic sediments (silty clays) as discussed in the text and in Lawson et al. (2014). The surface of the peatland is assumed to be flat.

Figure 3: Sedimentology of cores QT-2011-2, QT-2012-9, QT-2012-10 and QT-2012-18. Pollen assemblage zones (PAZ) are indicated. See Figure 4 for legend to Troels-Smith symbology.

Figure 4: Pollen percentage for selected taxa from cores QT-2011-2, QT-2012-9, QT-2012-10 and QT-2012-18. Abbreviations: Comb., Combretaceae; Pap., Papilionaceae; PAZ, pollen assemblage zones; t., type; undiff., undifferentiated.

Figure 5: *Mauritia*-type grain sizes and pollen and phytolith concentrations for cores QT-2011-2, QT-2012-9, QT-2012-10 and QT-2012-18. The number of *Mauritia*-type grains measured in each sequence (*n*) is indicated; where more than four grains were measured in a sample, the standard error of the mean is indicated by a horizontal bar. Pollen assemblage zones (PAZ) are indicated. See Figure 4 for legend to Troels-Smith symbology.

Figure 6: Pollen percentage for selected taxa from cores QT-2010-1 (Roucoux et al., 2013) and QT-2010-3 (Kelly et al., 2018). Abbreviations: Comb., Combretaceae; Pap., Papilionaceae; PAZ, pollen assemblage zones; t., type; undiff., undifferentiated.

Figure 7: NMDS biplots for the six pollen records from Quistococha, and the location of taxa in the same space. In each biplot the lowermost sample is indicated by a circle and the

991 uppermost by a square; the samples are linked in stratigraphic order by a line. The taxa shown
992 in Figures 4 and 6 were amalgamated to family level before analysis, except members of the
993 Arecaceae. Abbreviations: Cecrop., Cecropiaceae; Melastom.,
994 Melastomataceae/Combretaceae undifferentiated.

995 **Figure 8:** Probability density functions for basal radiocarbon dates (grey) and for the main
996 increase in Mauritia-t pollen (black) for the Quistococha peat cores (including core QT-2010-
997 1 of Roucoux et al., 2013), plotted using OxCal (Bronk Ramsey, 1995; Bronk Ramsey & Lee,
998 2013). Dates have been arranged as a transect, with basal dates from the north of the site at the
999 top and from the south of the site at the bottom. The grey band shows the range of the initiation
1000 dates for the area within 800 m of the lake (Phase I), and the blue band shows the (Phase II)
1001 dates from cores on the more southerly parts of the site. Inset map shows the position of all the
1002 cores taken, with radiocarbon-dated cores marked in black. The green band encompasses the
1003 period of *Mauritia*-t expansion.

1004

Figures

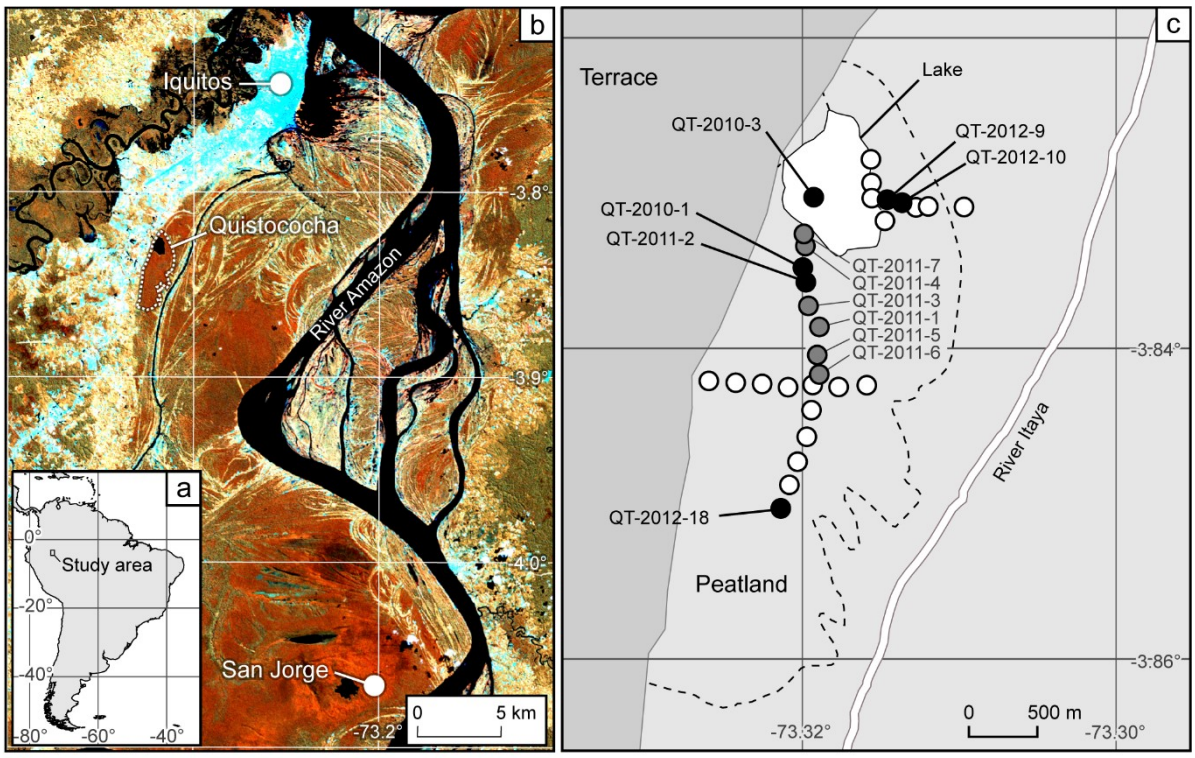

Figure 1

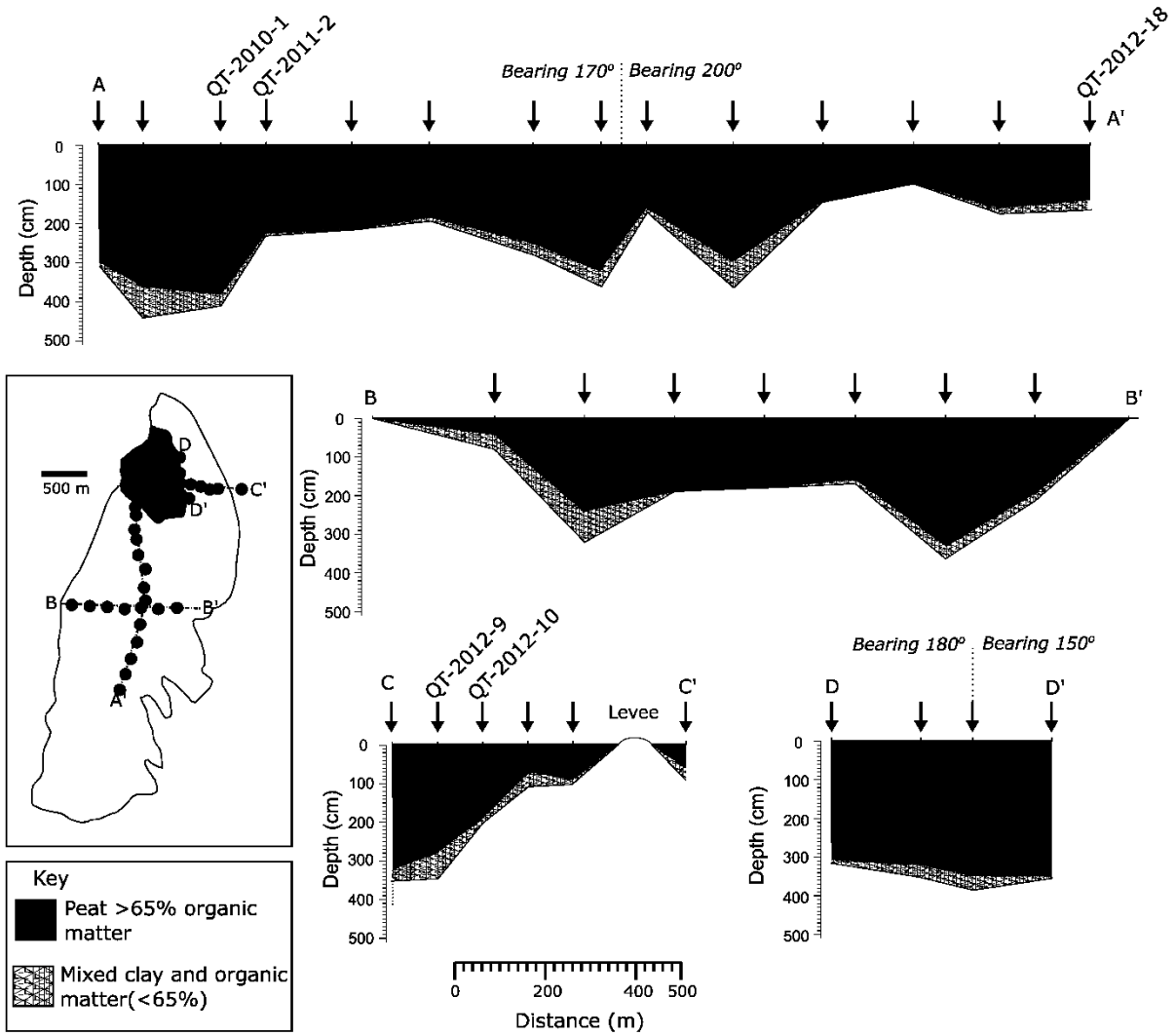
A
QT-2010-1
QT-2011-2
Bearing 170°
Bearing 200°
QT-2012-18
A'
Depth (cm)
0
100
200
300
400
500
500 m
D
C'
D'
B
B'
A
B
B'
C
QT-2012-9
QT-2012-10
Levee
C'
Bearing 180°
Bearing 150°
D
D'
0
200
400
500
Distance (m)
Key
Peat >65% organic matter
Mixed clay and organic matter(<65%)

Figure 2

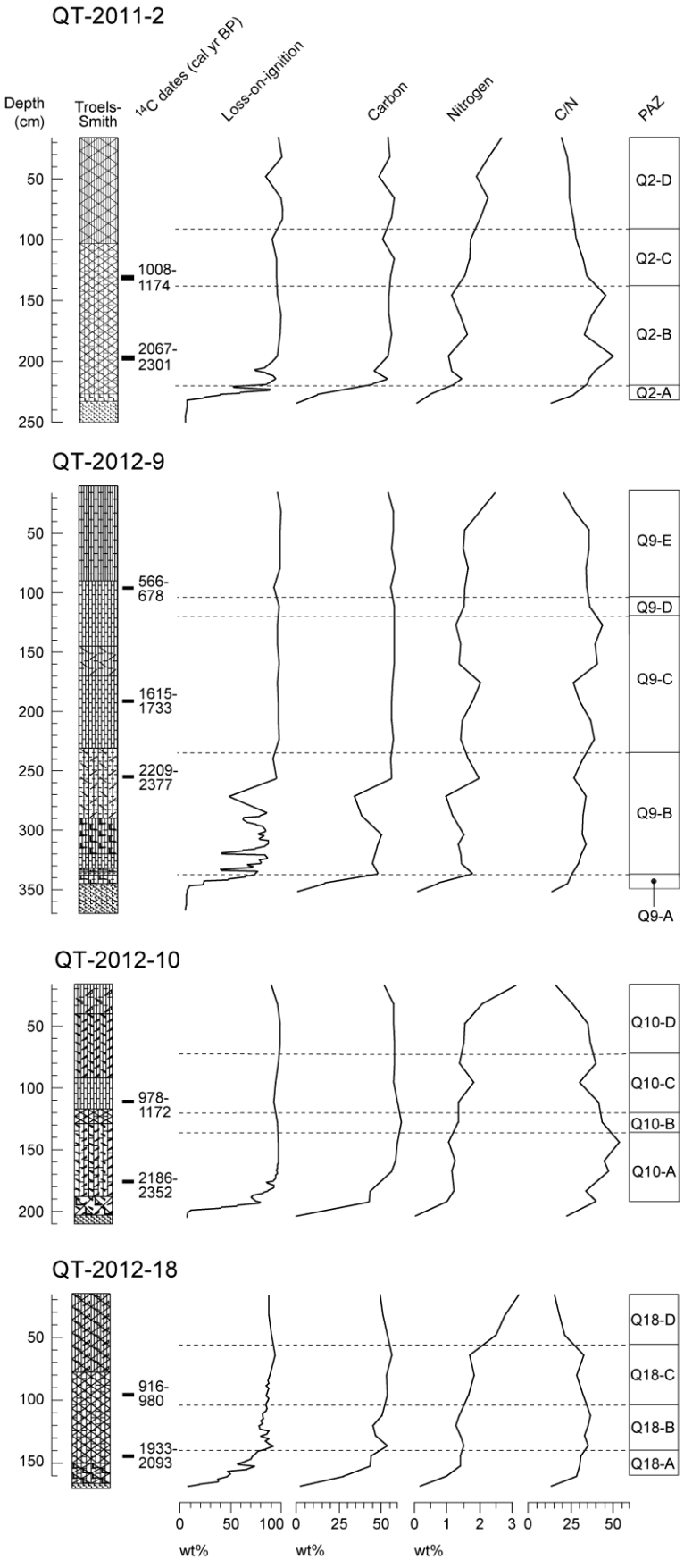
QT-2011-2
Depth (cm)
Troels-Smith
14C dates (cal yr BP)
Loss-on-ignition
Carbon
Nitrogen
C/N
PAZ
50
100
150
200
250
1008-1174
2067-2301
Q2-D
Q2-C
Q2-B
Q2-A
QT-2012-9
50
100
150
200
250
300
350
566-678
1615-1733
2209-2377
Q9-E
Q9-D
Q9-C
Q9-B
Q9-A
QT-2012-10
50
100
150
200
978-1172
2186-2352
Q10-D
Q10-C
Q10-B
Q10-A
QT-2012-18
50
100
150
916-980
1933-2093
Q18-D
Q18-C
Q18-B
Q18-A
0 50 100
wt%
0 25 50
wt%
0 1 2 3
wt%
0 25 50

Figure 3

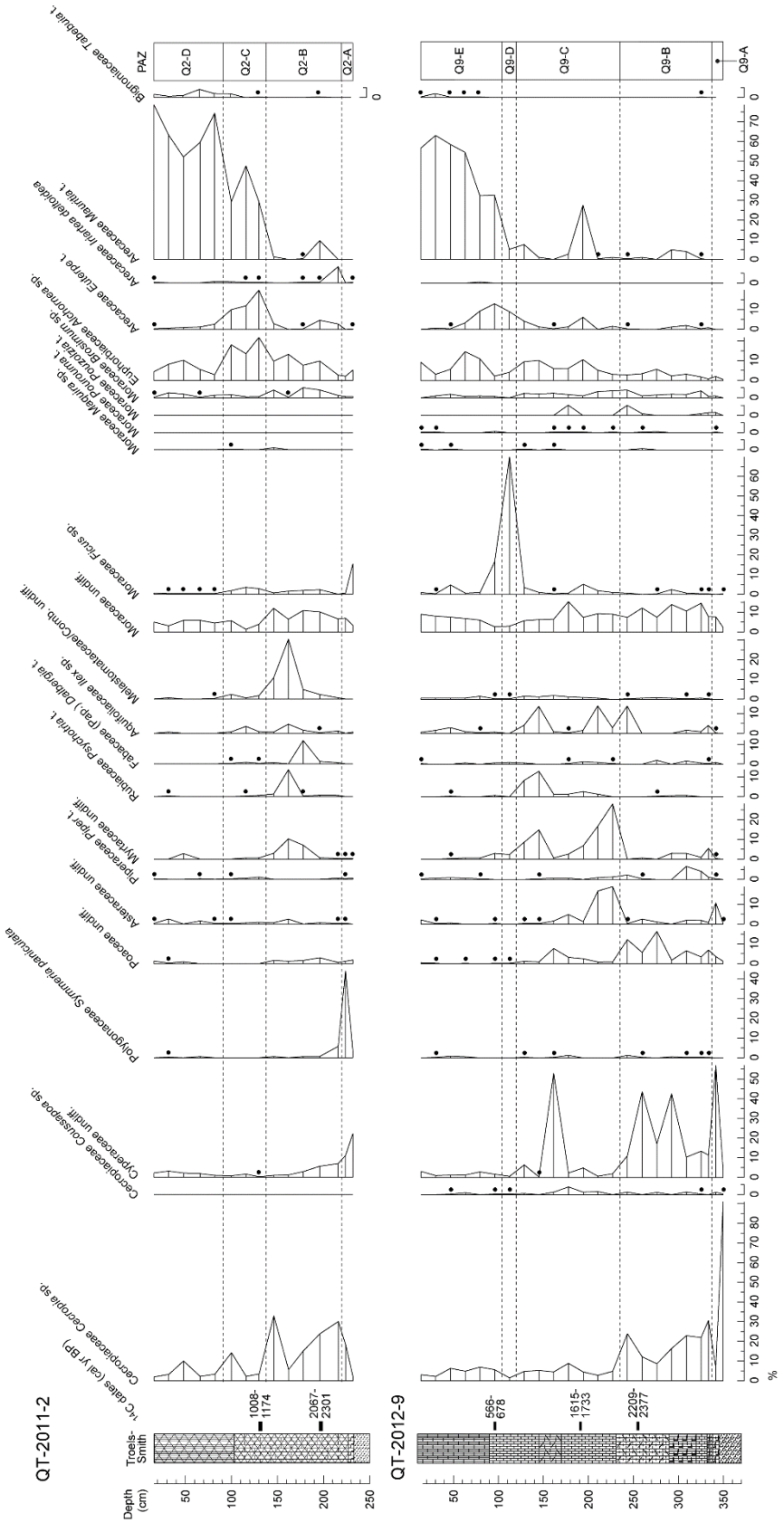

Figure 4 (part 1)

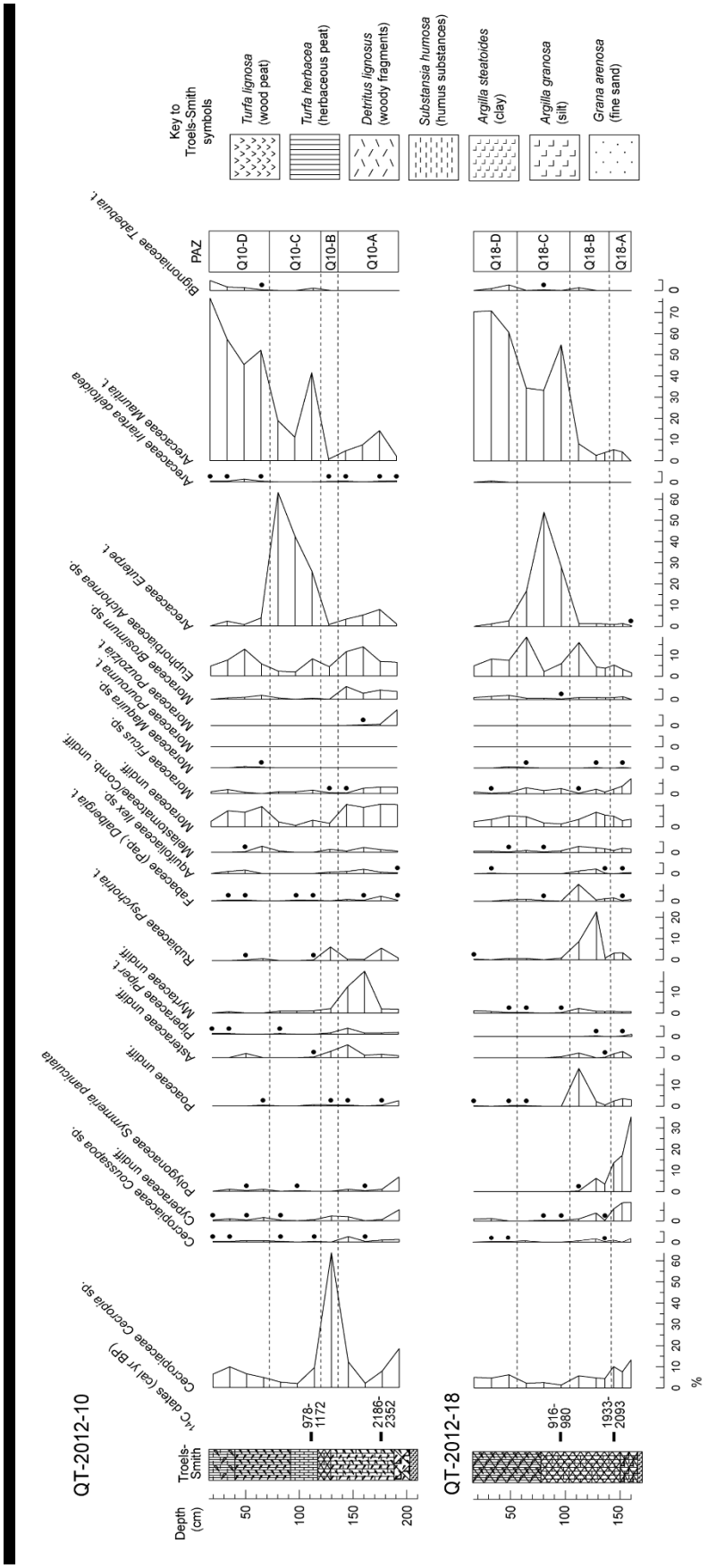

Figure 4 (part 2)

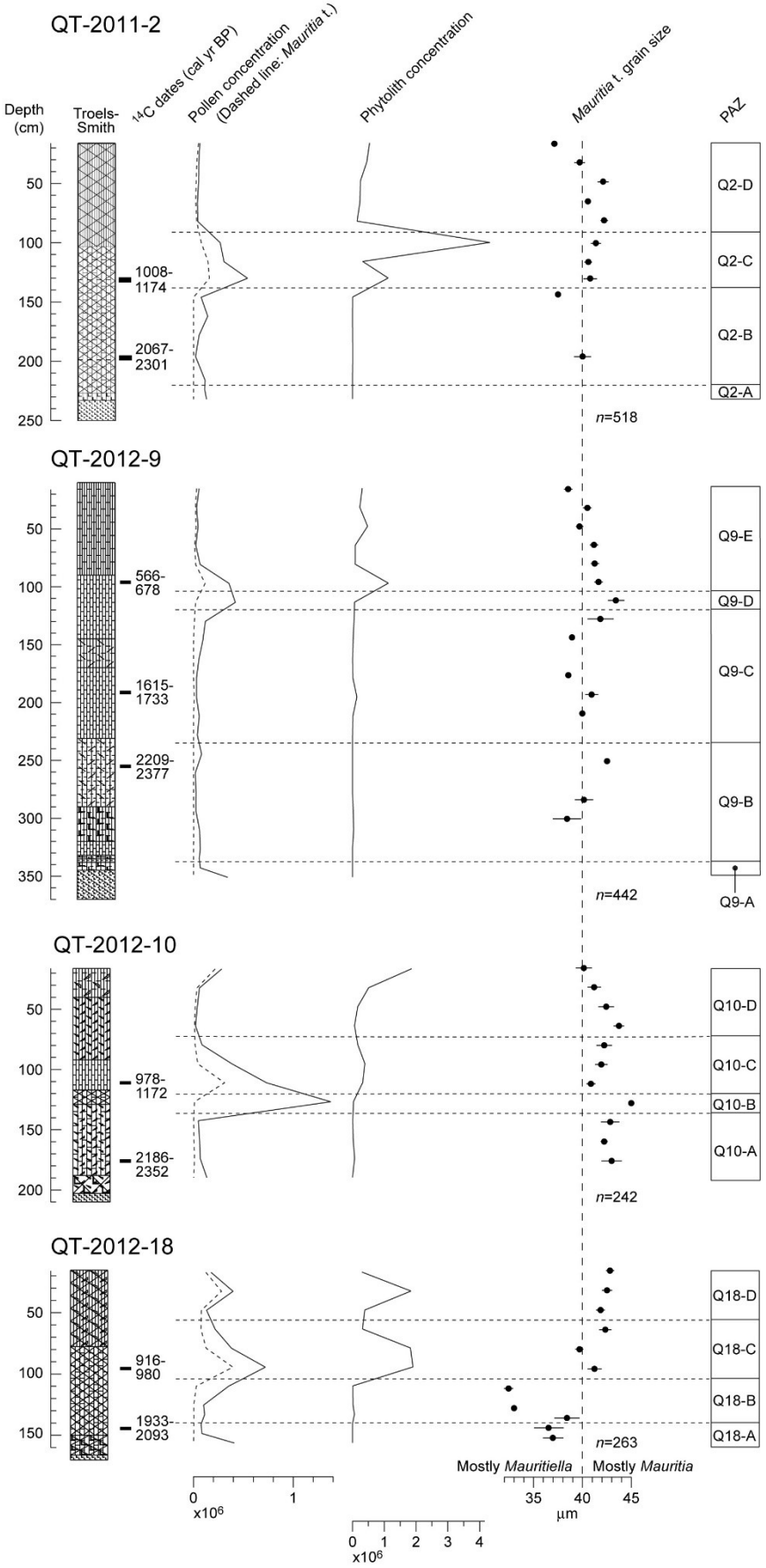
QT-2011-2
Depth (cm)
Troels-Smith
14C dates (cal yr BP)
Pollen concentration (Dashed line: Mauritia t.)
Phytolith concentration
Mauritia t. grain size
PAZ
50
100
150
200
250
1008-1174
2067-2301
Q2-D
Q2-C
Q2-B
Q2-A
n=518
QT-2012-9
50
100
150
200
250
300
350
566-678
1615-1733
2209-2377
Q9-E
Q9-D
Q9-C
Q9-B
Q9-A
n=442
QT-2012-10
50
100
150
200
978-1172
2186-2352
Q10-D
Q10-C
Q10-B
Q10-A
n=242
QT-2012-18
50
100
150
916-980
1933-2093
Q18-D
Q18-C
Q18-B
Q18-A
n=263
Mostly Mauritiella
Mostly Mauritia
0
1
x10⁶
35
40
45
µm
0
1
2
3
4
x10⁶

Figure 5

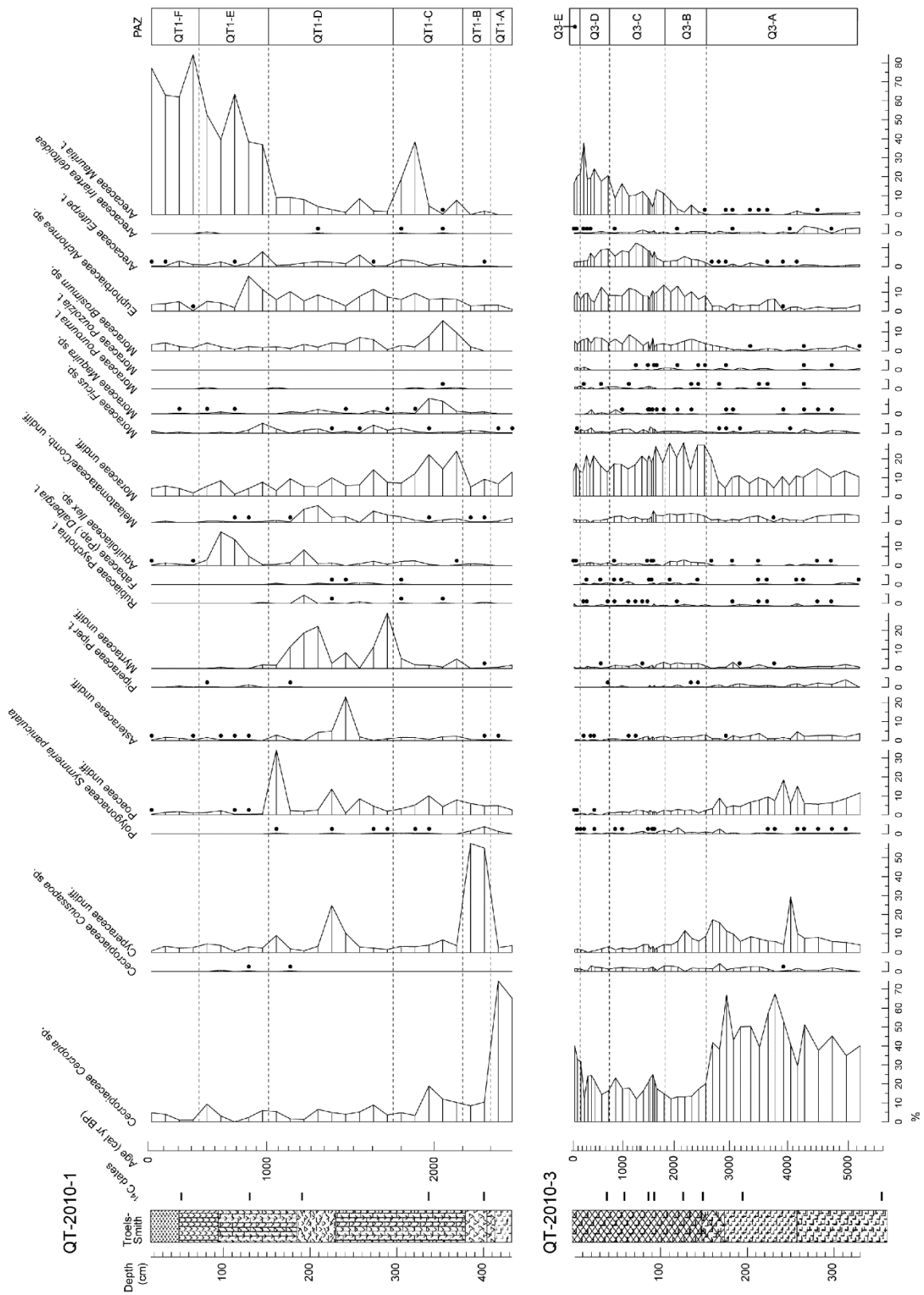
PAZ
QT1-F
QT1-E
QT1-D
QT1-C
QT1-B
QT1-A
Q3-E
Q3-D
Q3-C
Q3-B
Q3-A
Cecropiaceae Cecropia sp.
Cecropiaceae Coussapoa sp.
Cyperaceae undiff.
Polygonaceae Symmeria paniculata
Poaceae undiff.
Asteraceae undiff.
Piperaceae Piper t.
Myrtaceae undiff.
Rubiaceae Psychotria t.
Fabaceae (Pap.) Dalbergia t.
Aquifoliaceae Ilex sp.
Melastomataceae/Comb. undiff.
Moraceae undiff.
Moraceae Ficus sp.
Moraceae Maquira sp.
Moraceae Pourouma t.
Moraceae Pouteria t.
Moraceae Brosimum t.
Euphorbiaceae Alchornea sp.
Arecaceae Euterpe t.
Arecaceae Iriartea deltoidea
Arecaceae Mauritia t.
Depth (cm)
Troels-Smith
^{14}C dates
Age (cal yr BP)
QT-2010-1
QT-2010-3
%

Figure 6

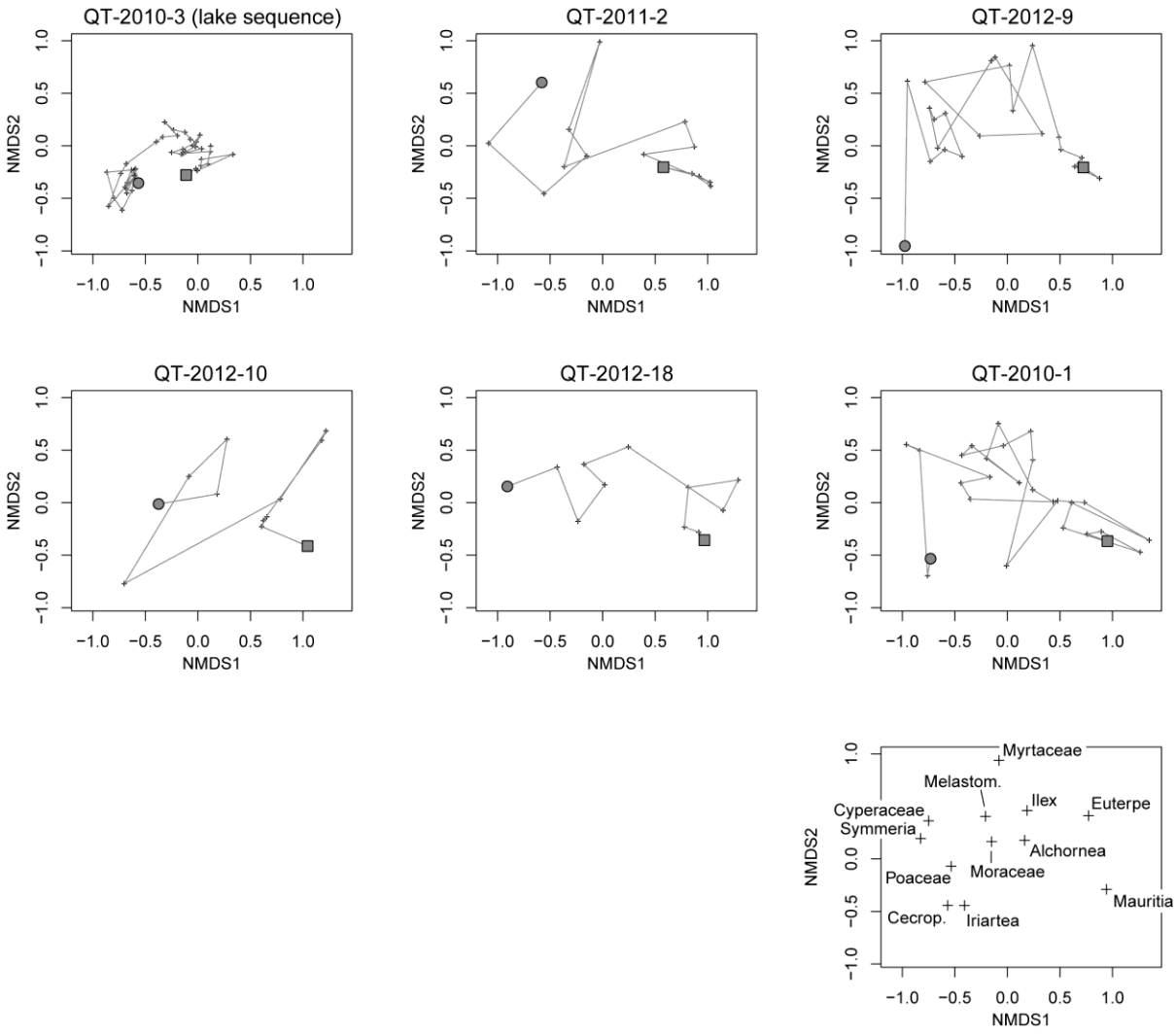
QT-2010-3 (lake sequence)
QT-2011-2
QT-2012-9
QT-2012-10
QT-2012-18
QT-2010-1
NMDS1
NMDS2
Myrtaceae
Melastom.
Ilex
Euterpe
Cyperaceae
Symmeria
Alchornea
Poaceae
Moraceae
Mauritia
Cecrop.
Iriartea

Figure 7

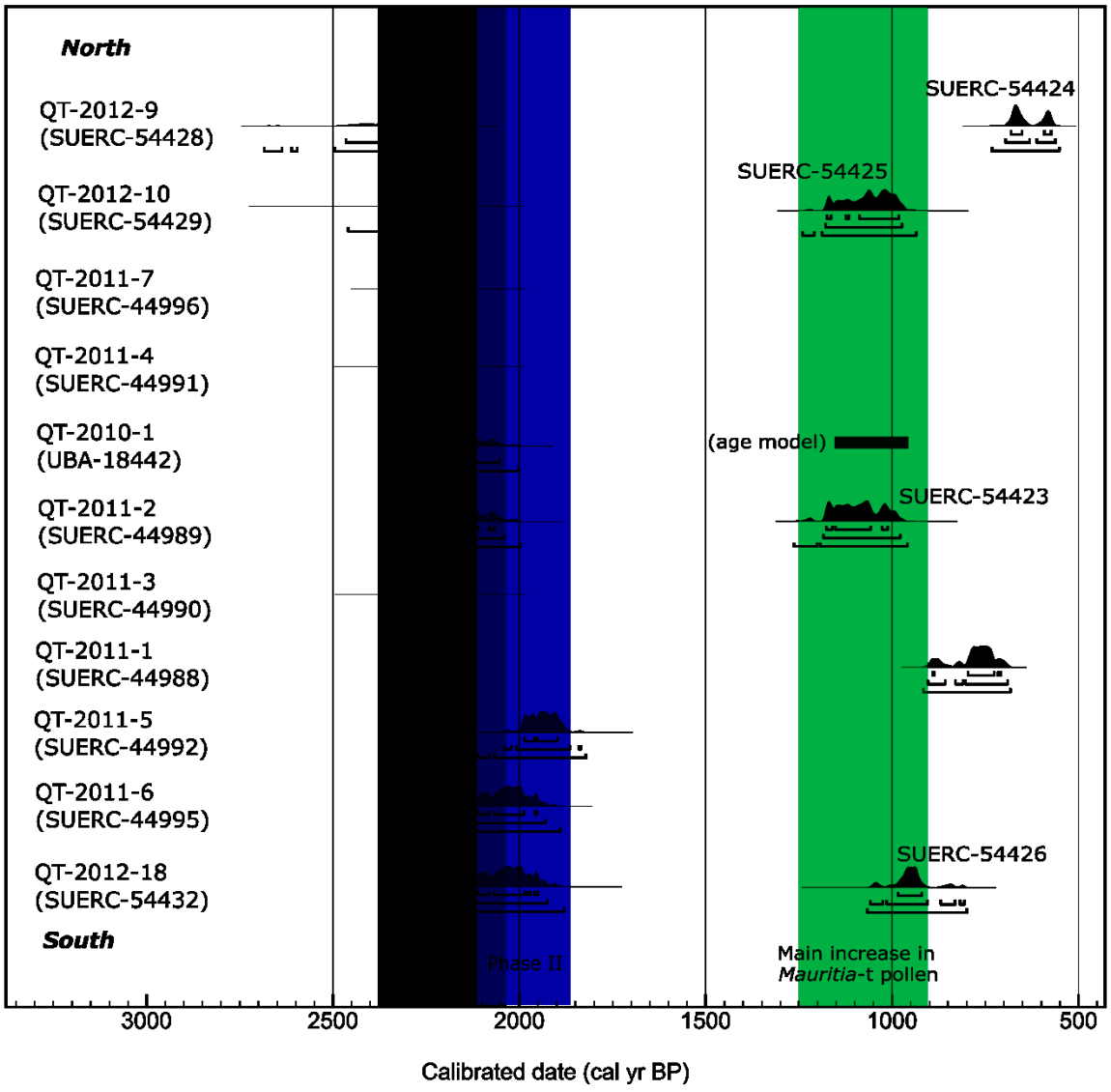
North
QT-2012-9
(SUERC-54428)
QT-2012-10
(SUERC-54429)
QT-2011-7
(SUERC-44996)
QT-2011-4
(SUERC-44991)
QT-2010-1
(UBA-18442)
QT-2011-2
(SUERC-44989)
QT-2011-3
(SUERC-44990)
QT-2011-1
(SUERC-44988)
QT-2011-5
(SUERC-44992)
QT-2011-6
(SUERC-44995)
QT-2012-18
(SUERC-54432)
South
SUERC-54424
SUERC-54425
(age model)
SUERC-54423
SUERC-54426
Phase II
Main increase in
Mauritia-t pollen
3000
2500
2000
1500
1000
500
Calibrated date (cal yr BP)

Figure 8